ACS Chemical Neuroscience

Research Article

pubs.acs.org/chemneuro

Novel 1-Phenyl-3-hydroxy-4-pyridinone Derivatives as Multifunctional Agents for the Therapy of Alzheimer's Disease

Rong Sheng,*[,†,#] Li Tang,[†,#] Liu Jiang,[†] Lingjuan Hong,[‡] Ying Shi,[‡] Naiming Zhou,[‡] and Yongzhou Hu*[,†]

[†]College of Pharmaceutical Sciences, Zhejiang University, Hangzhou, Zhejiang 310058, China

[‡]College of Life Sciences, Zhejiang University, Hangzhou, Zhejiang 310058, China

Supporting Information

ABSTRACT: A series of novel 1-phenyl-3-hydroxy-4-pyridinone derivatives were designed and synthesized as multifunctional agents for Alzheimer's disease (AD) therapy through incorporation of 3-hydroxy-4-pyridinone moiety from deferiprone into the scaffold of H_3 receptor antagonists. Most of these new compounds displayed designed quadruple functions, H_3 receptor antagonism, Aβ aggregation inhibition, metal ion chelation, and radical scavenging. Especially, the most promising compound **5c** displayed nanomolar IC_{50} values in H_3 receptor antagonism with high selectivity, efficient capability to interrupt the formation of Aβ_{1-42} fibrils, good copper and iron chelating properties, and more potent 2,2′-azinobis(3-ethyl-benzothiazoline-6-sulfonic acid) radical cation ($ABTS^{\bullet+}$) scavenging activity than Trolox. Further biological evaluation revealed that it did not show obvious cytotoxicity and hERG potassium channel inhibition at micromolar concentration. In addition, compound **5c** demonstrated suitable pharmacokinetic properties and acceptable blood−brain barrier (BBB) permeability *in vivo*. All these results indicate that compound **5c** is a potential multifunctional candidate for AD therapy.

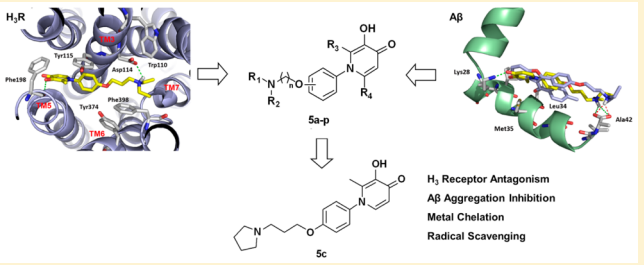

KEYWORDS: *Multifunctional agents, H_3R antagonism, Aβ aggregation inhibition, radical scavenge, metal ion chelation, Alzheimer's disease*

Alzheimer's disease (AD) is the most common form of dementia characterized by progressive memory loss and cognitive impairments.[1] It afflicts more than 24 million people worldwide with the trend of increasing.[2,3] Although the exact etiology of AD is not fully known, there are diverse factors that seem to play vital roles in the pathophysiology of the disease, including β-amyloid (Aβ) deposits, tau protein hyperphosphorylation, metal ion dyshomeostasis, oxidative stress, and neurotransmitter system dysfunction.[4−8] Currently, treatments for AD are acetylcholinesterase (AChE) inhibitors and the *N*-methyl-D-aspartate receptor antagonist, memantine. These therapies only achieve limited clinical efficacy in symptomatic improvement but fail to address the underlying causes of the disease.[9−11] Considering the complex pathogenesis of AD, multifunctional agents that simultaneous interfere with two or more causes of AD may achieve better therapeutic efficacy with complementary mechanisms of action.[12,13]

The H_3 receptor is an auto- and heteroreceptor that negatively regulates the release of histamine and several cognition-related key neurotransmitters, such as acetylcholine, serotonin, noradrenaline, and dopamine.[14−16] H_3 receptor antagonists can increase these neurotransmitter levels in the brain and may benefit patients with AD, Parkinson's disease, and other neurodegenerative diseases.[17] In recent years, several selective H_3 receptor antagonists have been evaluated in clinical trials as therapeutic candidates for AD, such as ABT-288, AZD5213, CEP-26401, GSK239512, and MK0249 (Figure 1).[18]

The widely accepted amyloid hypothesis declared that the assembly of Aβ into oligomers and fibrils is one of the central events in the progression of AD.[5,19−22] Various reports also confirmed that the aggregated Aβ species are toxic to neuronal cells *in vitro* and *in vivo*, which make it reasonable to develop Aβ aggregation inhibitors as potential AD therapeutic agents.[21,23] In addition, biometal dyshomeostasis maybe involved in this Aβ aggregation process and contributes to the neuronal dysfunction of AD. The most direct proof is that remarkably high concentrations of copper, zinc, and iron ions have been found to colocalize with the amyloid deposits in the AD-affected brain.[24−26] On the other hand, redox active iron and copper ions can lead to the generation of reactive oxygen species (ROS), which may result in oxidative damage to biological molecules and trigger neurodegeneration.[24,27] Therefore, blocking metal-induced Aβ aggregation and reducing oxidative stress offers an alternative approach to AD treatment. The metal chelator clioquinol (CQ) has been evaluated in clinical trials for the treatment of AD patients with positive results,[28] and its analogue PBT2 also has been advanced into clinical trials (Figure 1).[29]

Received: August 18, 2015
Accepted: October 19, 2015
Published: October 19, 2015

DOI: 10.1021/acschemneuro.5b00224
ACS Chem. Neurosci. 2016, 7, 69−81

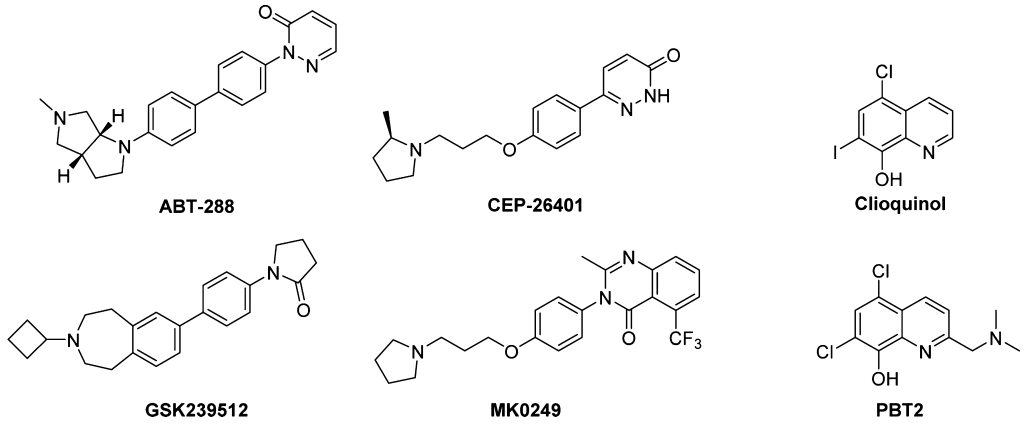

Figure 1. Structures of selected H_3 antagonists and metal chelators in clinical trials.

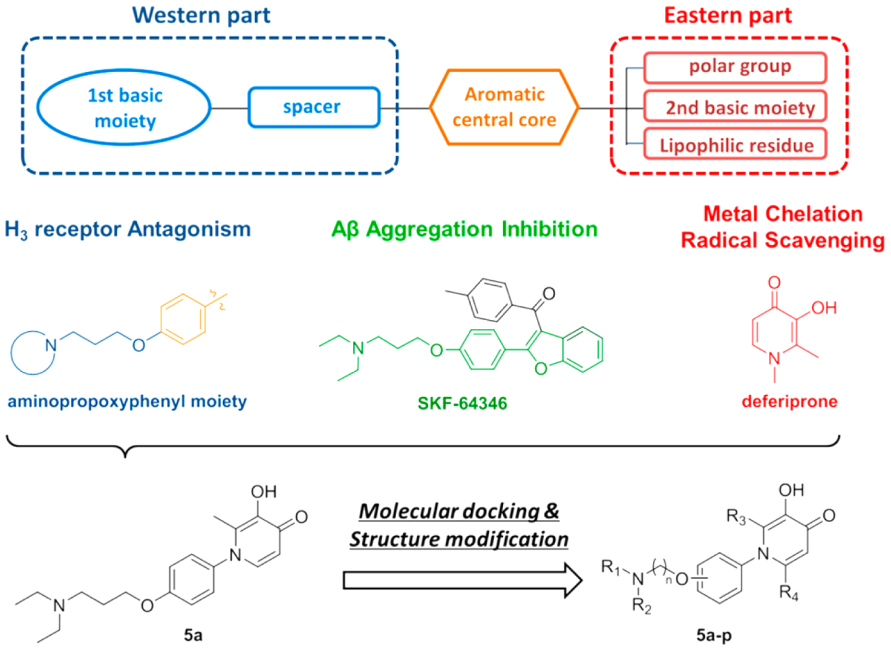

Figure 2. Rational design of 1-phenyl-3-hydroxy-4-pyridinone derivatives as multifunctional agents.

In our previous work, a series of indole derivatives were designed and synthesized as H_3 receptor antagonists and radical scavengers.[30] As a continuation of this work, we present here a series of 1-phenyl-3-hydroxy-4-pyridinone derivatives (**5a**−**p**) as the first class of multifunctional agents integrating H_3 receptor antagonism, anti-Aβ aggregation, metal chelation, and radical scavenging activities into one molecule.

RESULTS AND DISCUSSION

Rational Design of Multifunctional Ligands. To develop a drug candidate capable of targeting multiple AD pathological factors, we undertook a rational pharmacophore-directed design (Figure 2).

The generally accepted pharmacophore model of H_3 receptor antagonists is composed of a "western part" containing a tertiary basic amine and a spacer, an aromatic central core, and an "eastern part" consisting of either a polar group, a second basic amine, or a lipophilic residue.[31] On the basis of information in the literature and our previously obtained insights into the binding mode with H_3 receptors, the aminopropoxyphenyl moiety,[31,32] a critical pharmacophore acting as the "western part" and the central core to attain potent H_3 receptor antagonistic activity was chosen as a building block for our novel molecules. Thus, we prioritized the introduction of an appropriate metal chelating pharmacophore as the "eastern part" to generate novel hybrids with multiple functions. The 3-hydroxy-4-pyridinone moiety of marketed metal chelator deferiprone was chosen due to its desirable chelating properties with high affinity for copper, zinc, and iron ions but low affinity for sodium, potassium, magnesium, and calcium ions,[33] as well as its potential radical scavenging activity.[34,35] Interestingly, the newly designed 1-phenyl-3-hydroxy-4-pyridinone derivatives share similar structural elements to Aβ aggregation inhibitor SKF-64346 (amino-propyloxy-phenyl-benzofuran moiety).[36] Thus, the structure of compound **5a** was established through incorporating the 2-methyl-3-hydroxy-4-pyridinone moiety from deferiprone into the structure of SKF-64346.

To confirm the rationality of our design strategy, molecular docking simulations of **5a** with H_3 receptor homology model (based on H_1 receptor crystal structure, PDB ID 3RZE[37]) and monomeric Aβ_{1-42} (PDB ID 1IYT[38]) were performed (Figure

DOI: 10.1021/acschemneuro.5b00224
ACS Chem. Neurosci. 2016, 7, 69−81

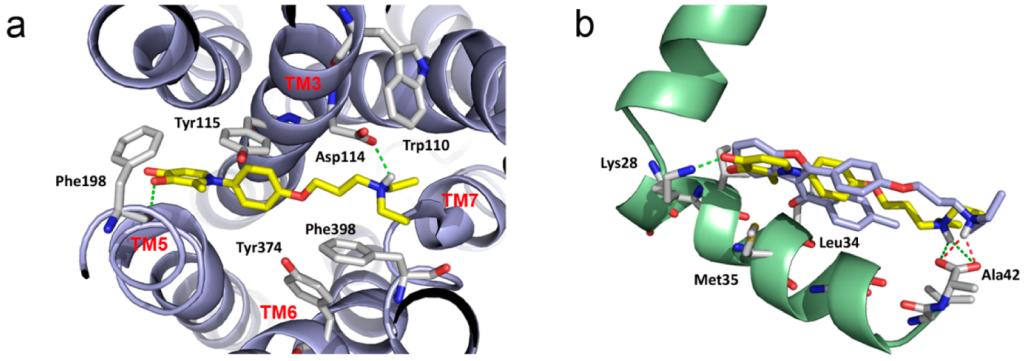

Figure 3. Docking study of **5a** with H_3 receptor homology model and monomeric Aβ_{1-42}. (**5a**, yellow sticks; SKF-64346, blue sticks; the dashed lines indicate possible hydrogen-bond contacts): (a) binding pattern of **5a** with H_3R homology mode; (b) binding pattern of **5a** and SKF-64346 with Aβ_{1-42}.

Scheme 1. Synthetic Route to Compounds 5a−p[a]

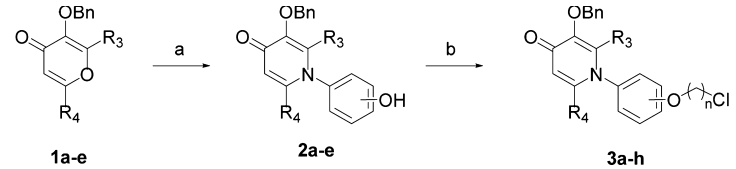

1a-e **2a-e** **3a-h**

1a: R_3= CH_3, R_4=H
1b: R_3= C_2H_5, R_4=H
1c: R_3= H, R_4=CH_3
1d: R_3= H, R_4=H

2a: *para*, R_3= CH_3, R_4=H
2b: *para*, R_3= C_2H_5, R_4=H
2c: *para*, R_3= H, R_4=CH_3
2d: *para*, R_3= H, R_4=H
2e: *meta*, R_3= CH_3, R_4=H

3a: *para*, R_3= CH_3, R_4=H, n=3
3b: *para*, R_3= C_2H_5, R_4=H, n=3
3c: *para*, R_3= H, R_4=CH_3, n=3
3d: *para*, R_3= H, R_4=H, n=3
3e: *meta*, R_3= CH_3, R_4=H, n=3
3f: *para*, R_3= CH_3, R_4=H, n=2
3g: *para*, R_3= CH_3, R_4=H, n=4
3h: *para*, R_3= CH_3, R_4=H, n=5

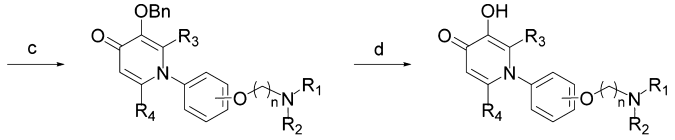

4a-p **5a-p**

4a, 5a: *para*, R_3= CH_3, R_4=H, n=3, NR_1R_2= diethylamino
4b, 5b: *para*, R_3= CH_3, R_4=H, n=3, NR_1R_2= dimethylamino
4c, 5c: *para*, R_3= CH_3, R_4=H, n=3, NR_1R_2= pyrrolidinyl
4d, 5d: *para*, R_3= CH_3, R_4=H, n=3, NR_1R_2= piperidinyl
4e, 5e: *para*, R_3= CH_3, R_4=H, n=3, NR_1R_2= morpholinyl
4f, 5f: *para*, R_3= CH_3, R_4=H, n=3, NR_1R_2= N-methylpiperazinyl
4g, 5g: *para*, R_3= C_2H_5, R_4=H, n=3, NR_1R_2= diethylamino
4h, 5h: *para*, R_3= C_2H_5, R_4=H, n=3, NR_1R_2= pyrrolidino

4i, 5i: *para*, R_3= H, R_4=CH_3, n=3, NR_1R_2= diethylamino
4j, 5j: *para*, R_3= H, R_4=CH_3, n=3, NR_1R_2= pyrrolidinyl
4k, 5k: *para*, R_3= H, R_4=H, n=3, NR_1R_2= diethylamino
4l, 5l: *para*, R_3= H, R_4=H, n=3, NR_1R_2= pyrrolidinyl
4m, 5m: *meta*, R_3= CH_3, R_4=H, n=3, NR_1R_2= pyrrolidinyl
4n, 5n: *para*, R_3= CH_3, R_4=H, n=2, NR_1R_2= pyrrolidinyl
4o, 5o: *para*, R_3= CH_3, R_4=H, n=4, NR_1R_2= pyrrolidinyl
4p, 5p: *para*, R_3= CH_3, R_4=H, n=5, NR_1R_2= pyrrolidinyl

[a]Reaction conditions: (a) 4-aminophenol or 3-aminophenol, 0.38 mol/L HCl solution, EtOH, microwave, 155 °C, yield 60−71%; (b) K_2CO_3, $Br(CH_2)_nBr$ or $Br(CH_2)_nCl$, n = 2−5, CH_3CN, reflux, yield 56−86%; (c) HNR_1R_2, triethylamine, CH_3CN, reflux, yield 68−82%; (d) 10% Pd/C, H_2, CH_3OH, rt, yield 96−99%.

3). The result reveals that compound **5a** has a favorable fit into a hydrophobic cavity in the TM 3−5−6−7 region of the H_3 receptor. The 3-hydroxy moiety of **5a** forms a hydrogen bond with the carbonyl of Phe198, and the phenyl ring is involved in a perpendicular $\pi-\pi$ interaction with the aromatic moiety of Tyr115. In addition, the protonated nitrogen of the diethylamino group produces a hydrogen bond with residue Asp114, which is critical for H_3 receptor activation.[39]

The molecular docking modes of the **5a** and SKF-64346 with Aβ_{1-42} monomer are shown in Figures 3c,d. Both **5a** and SKF-64346 are located near the C-terminus of Aβ_{1-42} and the protonated nitrogen forms a hydrogen bond with the oxygen of Ala42, which is similar to the previously reported binding mode by Li group.[40] Additionally, the carbonyl moiety of **5a** forms another hydrogen bond with the amino group of Lys28. The molecular docking results indicate that compound **5a** and SKF-64346 share the similar binding mode with Aβ_{1-42} and can inhibit Aβ_{1-42} aggregation by interfering with the formation of β-sheets.

To investigate the SAR of these newly designed compounds and find an optimal candidate for further development, structural modifications on compound **5a** were carried out. First, the diethylamino moiety of **5a** was replaced by different types of amines (dimethylamine, pyrrolidine, piperidine, morpholine, *N*-Me-piperazine) to search for the optimal basic center (compounds **5b−f**). Next, the R_3 and R_4 on the 3-hydroxy-4-pyridinone ring are modified with hydrogen, methyl or ethyl to evaluate their effect on multiple functions (compounds **5g−l**). Furthermore, the substitution position and the length of alkyloxy linker between phenyl and amino moiety were investigated to confirm the most favorable connection pattern for multiple functions (compounds **5m−p**). In these designed compounds, all the structural elements were selected to adhere to the values of Lipinski's rules and logBB for possible druglikeness (Table S1).

DOI: 10.1021/acschemneuro.5b00224
ACS Chem. Neurosci. 2016, 7, 69−81

Table 1. Biological Evaluation of Compounds 5a−p[a]

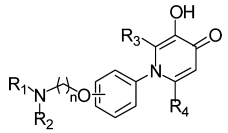

5a-p

Compd.	-NR1R2	R3	R4	Substitution pattern	n	hH3R IC50 (nM)	TEAC Values[b]	Inhibiton of Aβ1-42 aggregation (%)[c]	Aβ1-42 IC50 (μM)
5a		CH3	H	*para*	3	12.18±0.93	1.20±0.13	57.79±1.71	17.23±2.27
5b		CH3	H	*para*	3	82.99±2.88	1.04±0.09	50.19±3.42	20.9±1.58
5c		CH3	H	*para*	3	0.32±0.01	1.54±0.15	80.12±0.73	2.85±0.22
5d		CH3	H	*para*	3	0.32±0.03	1.42±0.14	86.01±0.96	3.76±0.32
5e		CH3	H	*para*	3	9.08±0.77	0.44±0.03	45.88±9.11	n.t.[d]
5f		CH3	H	*para*	3	48.68±1.01	1.75±0.03	35.10±3.37	n.t.[d]
5g		C2H5	H	*para*	3	10.96±0.84	0.71±0.10	58.38±4.03	15.89±1.97
5h		C2H5	H	*para*	3	0.53±0.02	0.78±0.11	79.52±1.06	3.32±0.15
5i		H	CH3	*para*	3	5.17±0.09	1.36±0.13	65.27±1.89	10.33±0.56
5j		H	CH3	*para*	3	3.78±1.05	2.62±0.17	74.17±3.16	4.94±0.18
5k		H	H	*para*	3	17.39±1.34	4.09±0.25	63.08±9.80	15.07±0.94
5l		H	H	*para*	3	3.97±0.19	3.08±0.04	74.16±8.50	4.71±0.29
5m		CH3	H	*meta*	3	63.62±3.54	1.68±0.31	41.11±4.10	n.t.[d]
5n		CH3	H	*para*	2	260.01±6.70	1.43±0.09	54.87±3.30	16.82±0.42
5o		CH3	H	*para*	4	6.55±0.22	1.30±0.24	79.50±2.59	2.07±0.19
5p		CH3	H	*para*	5	17.40±0.53	1.67±0.16	73.38±1.33	3.02±0.14
		Clobenpropit				1.06±0.12	-	-	n.t.[d]
		Trolox				-	1.00±0.05	-	n.t.[d]
		Curcumin				-	0.63±0.04	54.62±5.85	14.74±0.23

[a]The values are expressed as the mean ± SD of at least three independent measurements. [b]TEAC, Trolox-equivalent antioxidant capacity. TEAC values were expressed as Trolox equivalents calculated from the ratio of the slopes of the concentration−response curves of the antioxidant vs Trolox. [c]20 μM of compounds and 25 μM of $A\beta_{1-42}$ were used. [d]Not tested.

The synthetic route to compounds **5a−p** is outlined in Scheme 1. 3-Benzyloxy-4-pyranone derivatives (**1a−d**) were prepared according to published methods and used as starting materials.[41−43] Condensation of compounds **1a−d** with *para*- or *meta*-aminophenol under microwave irradiation provided compounds **2a−e**, followed by alkylation reaction with $Br(CH_2)_nBr$ or $Br(CH_2)_nCl$ affording compounds **3a−h**. Condensation of **3a−h** with the corresponding secondary amines yielded **4a−p**, which were debenzylated with 10% Pd/C under hydrogen atmosphere to furnish the target compounds **5a−p**.

H_3 Receptor Antagonism. The H_3 receptor antagonistic activities of compounds **5a−p** were evaluated in a LANCE time-resolved fluorescence resonance energy transfer (TR-

DOI: 10.1021/acschemneuro.5b00224
ACS Chem. Neurosci. 2016, 7, 69−81

FRET) assay, which was designed to measure cAMP produced upon modulation of adenylyl cyclase activity by H_3 receptors. Clobenpropit was used as reference compound. The results (Table 1) revealed that the majority of these newly designed compounds demonstrated excellent H_3 receptor antagonistic activities with nanomolar IC_{50} values; especially compounds **5c**, **5d**, and **5h** were more potent than clobenpropit with IC_{50} values of 0.32, 0.32, and 0.53 nM, respectively.

The preliminary SAR shows that the amino moiety at the end affects the activity of compounds significantly. Pyrrolidino- and piperidino-containing compounds were more potent than diethyl-, dimethyl-, piperazino-, and morpholino-containing compounds (**5c**, **5d** versus **5a**, **5b**, **5e**, **5f**), indicating that the lipophilic cyclic amine is more favorable in this position, which is consistent with the SAR of previous reported H_3 receptor antagonists.[32]

Next, compounds **5g**−**l** with different substituents on 4-pyridinone scaffold displayed excellent H_3 receptor antagonistic activities with IC_{50} values ranging from 0.53 to 17.39 nM, which are similar to that of compounds **5a** and **5c** (12.18 and 0.32 nM, respectively), suggesting that the modification of R_3 and R_4 with small moieties is tolerable for H_3 receptor antagonism.

Change of the substitution position and shorten the length of the alkyloxy linker resulted in dramatic decrease in activity; *meta*-aminopropyloxy substituted compound **5m** and *para*-aminoethyloxy compound **5n** only exhibited moderate activity with IC_{50} values of 63.62 and 260.01 nM, respectively. The compromised activities of compounds **5o** and **5p** (IC_{50} = 6.55 and 17.40 nM, respectively) suggested that the introduction of amino-butyloxy and amino-pentoxy linkers was detrimental for H_3 receptor antagonistic activities. All these results confirmed that the *para*-aminopropyloxy moiety is essential for the H_3 receptor antagonism.

Inhibition of Aβ Self-Aggregation. The ability of compounds **5a**−**5p** to inhibit $A\beta_{1-42}$ self-aggregation was investigated using a thioflavin T (ThT) fluorescence assay with curcumin as a reference compound.[44] As shown in Table 1, most of these compounds demonstrated excellent $A\beta_{1-42}$ self-aggregation inhibitory activities, and eight of them were more potent inhibitors (IC_{50} values ranging from 2.07 to 10.33 μM) than curcumin (IC_{50} = 14.74 μM). Interestingly, the SAR of **5a**−**p** on $A\beta_{1-42}$ self-aggregation inhibition is similar to that of H_3 receptor antagonism. Dramatically decreased activities of morpholine and piperazine derivatives **5e** and **5f** (45.88% and 35.10% inhibition in 20 μM, respectively) were observed in comparison with pyrrolidine and piperadine compounds **5c** and **5d** (80.12% and 86.01%, respectively), suggesting the importance of the lipophilic cyclic amine moiety for $A\beta_{1-42}$ aggregation inhibition. The modification of R_3 and R_4 moieties on the pyridinone scaffold is tolerable for $A\beta_{1-42}$ aggregation (**5h**, **5j**, and **5l** versus **5c**). The obviously decrease in activity of compound **5m** (41.11% inhibiton) also confirmed that the *para*-aminopropyloxy linker was optimal for $A\beta_{1-42}$ aggregation inhibition.

Trolox-Equivalent Antioxidant Capacity (TEAC) Assay. Reactive radical species have been identified to be closely related to AD,[27] and compounds that can decrease reactive radical species may exert potential therapeutic effects. The Trolox-equivalent antioxidant capacity (TEAC) assay was used to determine the radical scavenging ability of compounds **5a**−**p** according to a previously reported method.[45,46] This assay is based on the generation and detection of a blue-colored cation ($ABTS^{\bullet+}$, 2,2′-azino-bis(3-ethyl-benzothiazoline-6-sulfonic acid) radical cation) using the water-soluble analogue of vitamin E, Trolox, as a standard. TEAC values were expressed as Trolox equivalents calculated from the ratio of the slopes of the concentration−response curves or the antioxidant vs Trolox (TEAC value = 1.00).

As depicted in Table 1, most of these new compounds displayed excellent radical scavenging activity with TEAC values ranging from 0.44 to 4.09. The modification of R_3 and R_4 moieties in the pyridinone ring affects the antioxidant activity obviously; unsubstituted pyridinone derivative **5k** and **5l** displayed the most potent antioxidant activity with TEAC values of 4.09 and 3.08, respectively, while the 2-ethyl-pyridinone compounds **5g** and **5h** exhibited compromised activities in comparison with 2-methyl or 5-methylpyridinone compounds (**5a**, **5c** and **5i**, **5j**). The morpholine-containing compounds exhibited the weakest activity among all the compounds, indicating that the change of amino moiety at the end also affects the antioxidant capacity.

Metal Chelating Properties. The metal chelating activities of compounds **5a**−**p** with copper, zinc, and iron were measured by UV−vis spectroscopy using deferiprone and 3-benzyloxy-4-pyridinone derivative **4c** as positive and negative control. As expected, almost all the designed compounds displayed good metal chelating activities similar to deferiprone but compound **4c** did not. As shown in Figure S2 (Supporting Information), significant red shift was observed in UV−vis spectra when Cu^{2+}, Fe^{2+}, or Zn^{2+} was mixed with the compounds **5a**−**p** and deferiprone, indicating the formation of metal ion complex. These results confirmed that the 3-hydroxy-4-pyridinone moiety is essential for the metal chelating activity.

The Choice of Drug Candidate. Based on above biological evaluation results, compound **5c** was the most promising compound with excellent multiple functions (IC_{50} = 0.32 nM for H_3 receptor antagonism, TEAC value of 1.54 for $ABTS^{\bullet+}$ scavenging activity, IC_{50} value of 2.85 μM for Aβ self-aggregation inhibition, and potent chelating activities with copper, iron and zinc ions). Therefore, compound **5c** was chosen for further biological evaluation.

The Histamine Receptor Subtype Selectivity. There are four subtypes of histamine receptors (H_1R−H_4R) with distinct biological functions, and selectivity is an important issue for H_3 receptor antagonists. The antagonistic activities of compound **5c** against the other three subtypes of histamine receptors were evaluated using the CRE (cAMP-response elements)-driven luciferase assay with thioperamide as a control.[47] As shown in Table 2, compound **5c** did not show obvious antagonistic activities against H_1, H_2, and H_4 receptors.

hERG Inhibitory Activity. Many highly potent H_3 antagonists has been prevented from further development due to hERG (human ether-à-go-go-related gene) potassium channel inhibition.[48] Therefore, the hERG inhibitory activity of

Table 2. Histamine Receptor Subtype Selectivity and hERG Inhibition

compd	hH_1R (IC_{50}, μM)	hH_2R (IC_{50}, μM)	hH_4R (IC_{50}, μM)	hERG inhibition
5c	>10	>10	>10	5.7% ± 1.4% at 3.0 μM
thioperamide	>10	>10	0.67 ± 0.11	
cisapride				44.1% ± 1.5% at 30 nM

DOI: 10.1021/acschemneuro.5b00224
ACS Chem. Neurosci. 2016, 7, 69−81

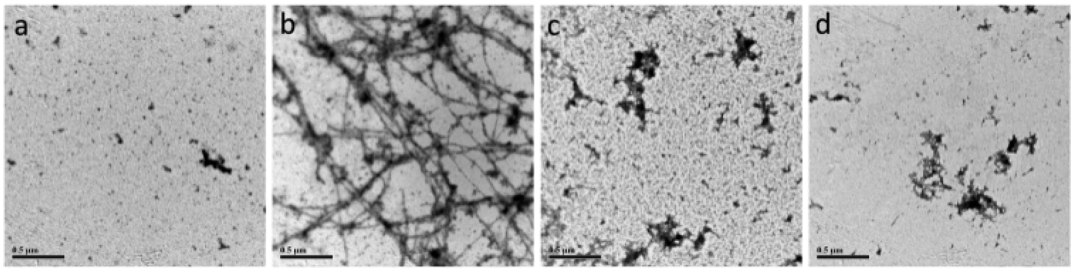

Figure 4. TEM images of Aβ_{1-42} self-mediated aggregation studies ([Aβ_{1-42}] = 25 μM, [compd] = 20 μM, 37 °C, 24 h, constant agitation, PBS, 50 000×): (a) Aβ 0 h; (b) Aβ; (c) Aβ + curcumin; (d) Aβ + **5c**.

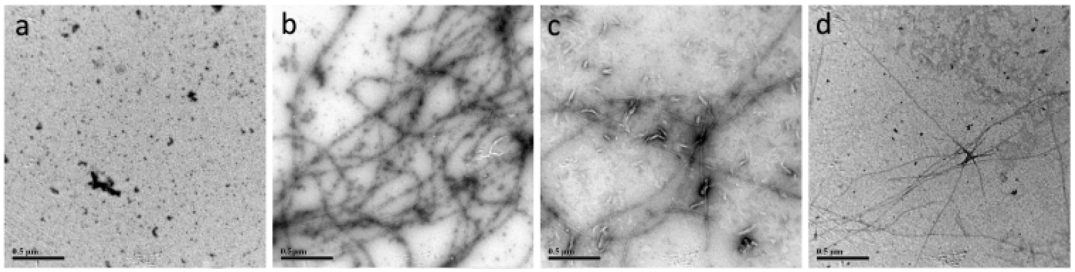

Figure 5. TEM images of Aβ_{1-42} species from disaggregation experiments ([Aβ_{1-42}] = 25 μM, [compd] = 20 μM, 37 °C, 24 h, constant agitation, PBS, 50 000×): (a) Aβ 0 h; (b) Aβ; (c) Aβ + curcumin; (d) Aβ+**5c**.

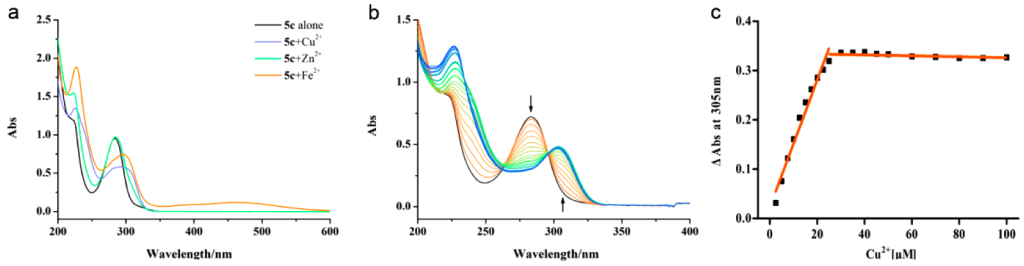

Figure 6. (a) The UV−vis spectra of compound **5c** with metal ions ([**5c**] = 50 μM, [M^{2+}] = 25 μM). (b) The UV−vis spectra of compound **5c** with Cu^{2+}. (c) Change in absorbance at 305 nm with increasing concentration of Cu^{2+} ([**5c**] = 50 μM, [Cu^{2+}] = 5−100 μM).

compound **5c** was detected by patch clamp assay using cisapride as a positive control. The results showed that **5c** only displayed 5.7% inhibition on hERG at 3.0 μM, while the cisapride exhibited 44.1% inhibition at 30 nM, indicating that **5c** possess very weak hERG potassium channel inhibition.

Inhibition of Self-Induced Aβ Aggregation. To further confirm that compound **5c** inhibits self-mediated Aβ_{1-42} aggregation, the inhibitory activity of compound **5c** was monitored by transmission electron microscopy (TEM) using curcumin as a control. In comparison with 0 h (Figure 4a), Aβ_{1-42} alone aggregated into well-defined amyloid fibrils after 24 h of incubation at 37 °C (Figure 4b). By contrast, only a few Aβ_{1-42} fibrils could be observed in the presence of curcumin or **5c** in the same conditions (Figure 4c,d).

Disaggregation of Self-Induced Aβ Aggregation. The ability of **5c** to disaggregate self-induced Aβ_{1-42} aggregation fibrils was also investigated using curcumin as positive control. Aβ_{1-42} fibrils were generated by incubating fresh Aβ_{1-42} for 24 h at 37 °C; curcumin or **5c** was then added to the sample and incubated for another 24 h at 37 °C with constant agitation. Figure 5c,d show that compound **5c** is capable of disassembling the Aβ fibrils from self-mediated aggregation with activity similar to that of curcumin.

Metal Chelating Properties of 5c. The UV−vis spectra of **5c** with different metal ions are shown in Figure 6a. When $CuCl_2$ was mixed with **5c**, the maximum absorption of **5c** at 283 nm exhibited a red shift to 305 nm and the minimum absorption shifted from 250 to 264 nm, indicating generation of a **5c**−Cu^{2+} complex. Addition of $FeSO_4$ to a solution of **5c** produced a similar maximum absorption wavelength shift, but addition of $ZnCl_2$ demonstrated only a weak minimum absorption shift. These data suggest that **5c** is a potent chelator for Cu^{2+} and Fe^{2+}, but not for Zn^{2+}.

In order to investigate the binding stoichiometry of **5c** with Cu^{2+}, spectrophotometric titrations were carried out.[49] A fixed amount of **5c** (50 μM) was mixed with increasing amounts of $CuCl_2$ (5−100 μM) and the absorbance changes at 305 nm (Figure 6b) were plotted. The presence of an isosbestic point indicated the formation of **5c**−Cu^{2+} complex and the intersection revealed a 2:1 **5c**−Cu^{2+} binding ratio, which was consistent with the results of 3-hydroxy-4-pyridone derivatives in the literature.[50] (Figure 6c).

Inhibition of Cu^{2+}-Induced Aβ Aggregation. To evaluate the ability of **5c** to inhibit Cu^{2+}-induced Aβ_{1-42} aggregation, the Th-T fluorescence and TEM experiments were carried out. For the ThT fluorescence assay (Figure S3), the Cu^{2+} lead to a reduced ThT fluorescence in comparison with Aβ alone (79.9%), probably due to the emission quenched by the paramagnetic Cu^{2+} ions inducing formation of nonfibrillar Aβ aggregates.[51,52] By contrast, the addition of **5c**

DOI: 10.1021/acschemneuro.5b00224
ACS Chem. Neurosci. 2016, 7, 69−81

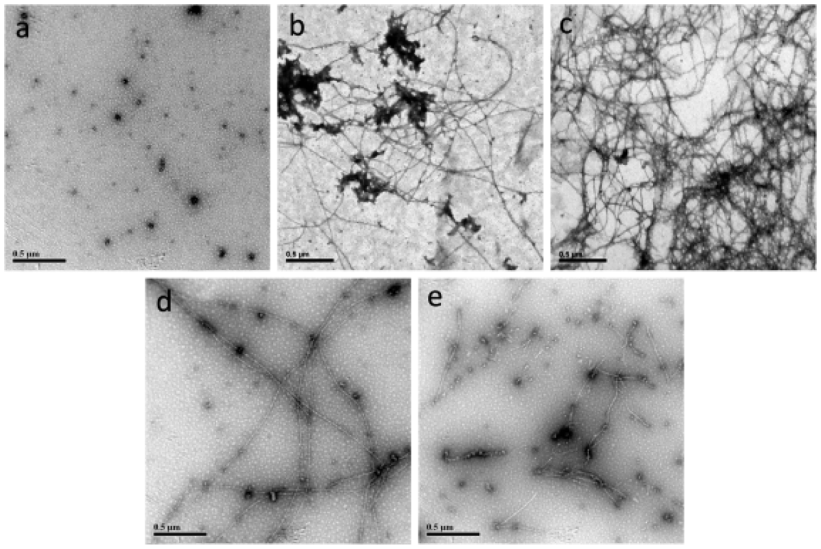

Figure 7. TEM image analysis of copper induced Aβ_{1-42} aggregation studies ([Aβ_{1-42}] = [Cu^{2+}] = 25 μM, [compd] = 50 μM, 37 °C, 24 h, constant agitation, HEPES, pH 6.6, 50 000×): (a) Aβ + Cu^{2+} 0 h; (b) Aβ; (c) Aβ + Cu^{2+}; (d) Aβ + Cu^{2+} + CQ; (e) Aβ + Cu^{2+} + **5c**.

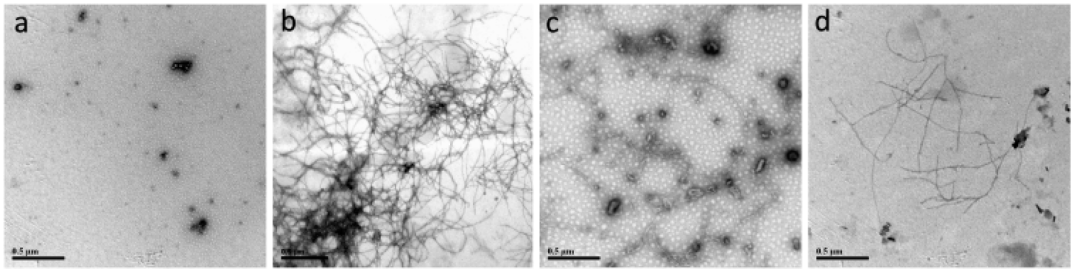

Figure 8. TEM image of disaggregation of copper induced Aβ_{1-42} aggregation ([Aβ_{1-42}] = [Cu^{2+}] = 25 μM, [compd] = 50 μM, 37 °C, 24 h, constant agitation, HEPES, pH 6.6): (a) Aβ + Cu^{2+} 0 h; (b) Aβ + Cu^{2+}; (c) Aβ + Cu^{2+} + CQ; (d) Aβ + Cu^{2+} + **5c**.

and CQ resulted in a dramatic decrease of ThT fluorescence (22.1% and 44.0% ,respectively), indicating their excellent activities to inhibit Cu^{2+} induced Aβ_{1-42} aggregation.

The TEM experiment shows that the aggregation of Aβ_{1-42} for 24 h at 37 °C leads to well-defined Aβ_{1-42} fibrils, and more complex Aβ fibrils were observed in the presence of copper ions than with Aβ_{1-42} alone (Figure 7b,c). As expected, noticeably fewer Aβ_{1-42} fibrils were observed when clioquinol (CQ) or **5c** was added to the samples (Figure 7d,e), indicating that **5c** can efficiently chelate the copper and inhibit copper-induced Aβ_{1-42} aggregation.

Disaggregation of Cu^{2+}-Induced Aβ Aggregation. The ability of **5c** to disaggregate copper-induced Aβ_{1-42} aggregation fibrils was examined using Th-T fluorescence assay and TEM as well. Aβ_{1-42} fibrils were generated by incubating fresh Aβ_{1-42} with 1.0 equiv of Cu^{2+} for 24 h at 37 °C with constant agitation (Figure 8b). Compound **5c** or clioquinol was then added to the sample and incubated for another 24 h at 37 °C.

As shown in Figure S4, the ThT binding assay demonstrated that both compound **5c** and clioquinol can disaggregate Aβ fibrils (57.9% and 46.6% disaggregation, respectively). The TEM assay also demonstrated that both clioquinol and **5c** can clearly disaggregate Aβ_{1-42} fibrils from Cu^{2+}-induced aggregation. (Figure 8c,d)

In Vitro Cytotoxicity. Orvig et al. reported that 3-hydroxy-4-pyridinone derivatives containing benzothiazole and benzoxazole functionality showed potent cytotoxicity similar to chemotherapeutic agent cisplatin.[53,54] These results limited the further development of these derivatives as AD therapeutic agents. In order to examine the potential cytotoxicity of our compounds, a SRB (sulforhodamine B) assay of **5c** against human glioma U251 cells was performed. As indicated in Figure 9, compound **5c** did not show obvious cytotoxicity at 20 μM after 24h incubation.

PK and BBB Penetration of 5c. A significant hindrance to the development of AD therapeutic agents is the relatively poor BBB penetration for many reported MTDL compounds.[55] To determine whether compound **5c** can penetrate BBB, plasma

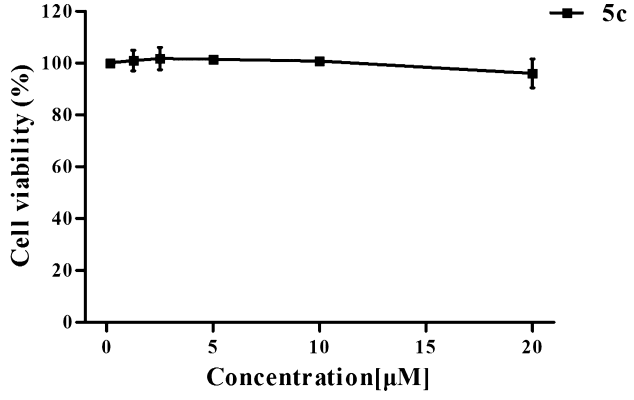

Figure 9. Effects of **5c** on U251 cell viability. Data represent mean ± SD.

DOI: 10.1021/acschemneuro.5b00224
ACS Chem. Neurosci. 2016, 7, 69−81

and brain pharmacokinetic (PK) studies were performed through intraperitoneal administration of **5c** (5 mg/kg) in male Sprague−Dawley rats. As summarized in Table 3,

Table 3. Pharmacokinetic Values of 5c in Male SD Rats[a]

ip (5 mg/kg)	plasma	brain
AUC_{0-3} (ng·h/mL)	512 ± 47	319 ± 45
$AUC_{0-\infty}$ (ng·h/mL)	636 ± 64	437 ± 135
$T_{1/2}$ (h)	1.6 ± 0.1	1.4 ± 0.5
Cl (mL/(min·kg))	132 ± 14	204 ± 66
V_d (L/kg)	18.7 ± 0.9	23.5 ± 2.5
T_{max} (h)	0.16 ± 0.02	0.4 ± 0.1
C_{max} (ng/mL)	771 ± 45	207 ± 2.5
B/P ratio[b]	0.69	

[a]Data are presented as the mean ± SD from three male SD rats. [b]B/P ratio is brain to plasma ratio calculated with $AUC_{0-\infty}$ exposure measured for brain and plasma tissues.

compound **5c** demonstrates acceptable exposure (636 ± 64 ng·h/mL), suitable half-life (1.6 ± 0.1 h), and high volumes of distribution (18.7 ± 0.9 L/kg) in the plasma. More importantly, compound **5c** achieves a mean C_{max} of 207 ng/mL in the brain within half an hour, and the brain/plasma exposure ratio was 0.69, which indicates that **5c** can efficiently cross the brain−blood barrier.

CONCLUSIONS

Through a combination of the metal chelating moiety 3-hydroxy-4-pydinone and the H_3 receptor antagonist pharmacophore moiety aminopropoxyphenyl into one molecule, a novel series of 1-phenyl-3-hydroxy-4-pyridinones **5a−p** have been designed, synthesized, and evaluated as potential AD therapeutic agents with multiple functions.

Among all the compounds, compound **5c** displayed excellent selective H_3 receptor antagonistic activity, efficient $ABTS^{\bullet+}$ scavenging effect, good copper and iron chelating properties, and effective inhibitory activity against self- and Cu^{2+}-induced $A\beta_{1-42}$ aggregation. Moreover, **5c** did not show obvious cytotoxicity against human glioma U251 cells or hERG inhibition risk in a patch clamp assay at micromolar concentration. More interestingly, an *in vivo* study revealed that **5c** possesses suitable PK profiles in plasma and acceptable BBB penetration behavior. Our research results suggest that this newly synthesized hybrid shows an interesting pharmacological profile against Alzheimer's disease. To the best of our knowledge, this is the first report of one compound possessing above four functions as a potential candidate for the treatment of AD; our work may provide an interesting strategy to design other multiple function agents with different mechanisms.

EXPERIMENTAL SECTION

General Methods. ^1H NMR spectra were recorded on an AVANCE II 400 M or AVANCE III 500 M spectrometer, ^{13}C NMR spectra were recorded on a 100 or 125 MHz spectrometer (chemical shifts are given in ppm relative to TMS as internal standard). Mass spectra (ESI-MS) were performed on an FINNIGAN LCQ-DECAXP spectrometer, and high-resolution mass spectra were performed on an Agilent 6224 TOF LC-MS spectrometer. Melting points were recorded on a B-540 Buchi melting-point apparatus and uncorrected. All final compounds were purified to ≥95% purity as determined by Agilent 1260 series HPLC systems with a YMC-Pack ODS-A C18 column (4.6 mm × 150 mm, 3 μm), 20.0 μL injection volume, flow rate of 1.0 mL/min, gradient of 5−50% B from 0 to 8 min, 50−95% B from 8 to 9 min, hold at 95% B from 9 to 10 min (mobile phase A, 0.1% formic acid in water, and mobile phase B, methanol) with a UV detector set at 290 nm.

General Synthetic Procedure for 2a−e. A mixture of 3-benzyloxy-4*H*-pyran-4-one derivative (**1a−d**; 10.0 mmol), aminophenol (22 mmol), 12.5 mL of 0.38 mol/L HCl solution, and 10.0 mL of ethanol was placed in a microwave tube containing a magnetic stirring bar. The reaction tube was sealed and irradiated in the cavity of a microwave apparatus at 155 °C for 15−20 min. After completion of the reaction, the tube was removed and cooled to room temperature, and the precipitate was filtered and rinsed with hot water to afford **2a−e**.

*3-Benzyloxy-1-(4-hydroxyphenyl)-2-methylpyridin-4(1H)-one (**2a**).* White solid, yield 65%. ^1H NMR (500 MHz, DMSO-d_6): δ 10.02 (s, 1H), 7.55 (d, *J* = 7.5 Hz, 1H), 7.44−7.42 (m, 2H), 7.39−7.36 (m, 2H), 7.34−7.31 (m, 1H), 7.19 (d, *J* = 9.0 Hz, 2H), 6.86 (d, *J* = 9.0 Hz, 2H), 6.21 (d, *J* = 7.5 Hz, 1H), 5.07 (s, 2H), 1.85 (s, 3H). ESI-MS: *m*/*z* = 308.4 $[M + H]^+$.

*3-Benzyloxy-2-ethyl-1-(4-hydroxyphenyl)pyridin-4(1H)-one (**2b**).* Pale-yellow solid, yield 68%. ^1H NMR (500 MHz, DMSO-d_6): δ 9.97 (s, 1H), 7.50 (d, *J* = 7.5 Hz, 1H), 7.45−7.43 (m, 2H), 7.39−7.36 (m, 2H), 7.33−7.31 (m, 1H), 7.24 (d, *J* = 9.0 Hz, 2H), 6.88 (d, *J* = 9.0 Hz, 2H), 6.21 (d, *J* = 7.5 Hz, 1H), 5.14 (s, 2H), 2.36−2.30 (q, *J* = 7.5 Hz, 2H), 0.80 (t, *J* = 7.5 Hz, 3H). ESI-MS: *m*/*z* = 322.3 $[M + H]^+$.

*5-Benzyloxy-1-(4-hydroxyphenyl)-2-methylpyridin-4(1H)-one (**2c**).* Pale-yellow solid, yield 71%. ^1H NMR (500 MHz, DMSO-d_6): δ 9.94 (s, 1H), 7.42−7.35 (m, 5H), 7.34−7.30 (m, 1H), 7.21 (d, *J* = 9.0 Hz, 2H), 6.88 (d, *J* = 9.0 Hz, 2H), 6.18 (d, *J* = 7.5 Hz, 1H), 4.95 (s, 2H), 1.94 (s, 3H). ESI-MS: *m*/*z* = 308.3 $[M + H]^+$.

*3-Benzyloxy-1-(4-hydroxyphenyl)pyridin-4(1H)-one (**2d**).* Pale-yellow solid, yield 60%. ^1H NMR (500 MHz, DMSO-d_6): δ 9.85 (s, 1H), 7.81 (dd, J_1= 7.5, J_2= 2.0 Hz, 1H), 7.72 (d, *J* = 2.0 Hz, 1H), 7.45−7.43 (m, 2H), 7.42−7.37(m, 2H), 7.36−7.33 (m, 3H), 6.89 (d, *J* = 9.0 Hz, 2H), 6.29 (d, *J* = 7.5 Hz, 1H), 5.06 (s, 2H). ESI-MS: *m*/*z* = 294.4 $[M + H]^+$.

*3-Benzyloxy-1-(3-hydroxyphenyl)-2-methylpyridin-4(1H)-one (**2e**).* White solid, yield 65%. ^1H NMR (500 MHz, DMSO-d_6): δ 10.09 (s, 1H), 7.58 (d, *J* = 7.5 Hz, 1H), 7.44−7.42 (m, 2H), 7.39−7.35 (m, 2H), 7.34−7.31 (m, 2H), 6.93−6.90 (m, 1H), 6.79−6.76 (m, 1H), 6.72 (t, *J* = 2.0 Hz, 1H), 6.23 (d, *J* = 7.5 Hz, 1H), 5.08 (s, 2H), 1.87 (s, 3H). ESI-MS: *m*/*z* = 308.4 $[M + H]^+$.

General Synthetic Procedure for 3a−h. A mixture of phenylpyridin-4(1*H*)-one derivative (**2a−e**; 5.0 mmol), K_2CO_3 (1.38g, 10.0 mmol), and $Br(CH_2)_nBr$ or $Br(CH_2)_nCl$, (10.0 mmol) was refluxed in 25 mL of acetonitrile for 6−8 h. The mixture was cooled to room temperature, filtered, washed with acetonitrile, and concentrated to dryness. The crude product was purified by silica gel chromatography to give pure **3a−h**.

*3-Benzyloxy-1-(4-(3-chloropropoxy)phenyl)-2-methylpyridin-4(1H)-one (**3a**).* Yellow solid, yield 56%. ^1H NMR (500 MHz, $CDCl_3$): δ 7.37−7.35 (m, 2H), 7.28−7.22 (m, 3H), 7.20 (d, *J* = 7.5 Hz, 1H), 7.02 (d, *J* = 9.0 Hz, 2H), 6.90 (d, *J* = 9.0 Hz, 2H), 6.49 (d, *J* = 7.5 Hz, 1H), 5.18 (s, 2H), 4.09 (t, *J* = 6.0 Hz, 2H), 3.70 (t, *J* = 6.0 Hz, 2H), 2.20−2.16 (m, 2H), 1.75 (s, 3H). ESI-MS: *m*/*z* = 384.2 $[M + H]^+$.

*3-Benzyloxy-1-(4-(3-chloropropoxy)phenyl)-2-ethylpyridin-4(1H)-one (**3b**).* Yellow solid, yield 69%. ^1H NMR (500 MHz, $CDCl_3$): δ 7.41−7.39 (m, 2H), 7.29−7.26 (m, 2H), 7.24−7.23 (m, 1H), 7.16 (d, *J* = 7.5 Hz, 1H), 7.10 (d, *J* = 9.0 Hz, 2H), 6.92 (d, *J* = 9.0 Hz, 2H), 6.46 (d, *J* = 7.5 Hz, 1H), 5.24 (s, 2H), 4.11 (t, *J* = 6.0 Hz, 2H), 3.72 (t, *J* = 6.0 Hz, 2H), 2.32 (q, *J* = 7.5 Hz, 2H), 2.23−2.18 (m, 2H), 0.78 (t, *J* = 7.5 Hz, 3H). ESI-MS: *m*/*z* = 398.3 $[M + H]^+$.

*5-Benzyloxy-1-(4-(3-chloropropoxy)phenyl)-2-methylpyridin-4(1H)-one (**3c**).* Yellow solid, yield 65%. ^1H NMR (500 MHz, $CDCl_3$): δ 7.33−7.31 (m, 2H), 7.27−7.23 (m, 2H), 7.23−7.20 (m, 1H), 7.01 (d, *J* = 9.0 Hz, 2H), 6.92 (s, 1H), 6.90 (d, *J* = 9.0 Hz, 2H), 6.34 (s, 1H), 5.06 (s, 2H), 4.10 (t, *J* = 6.0 Hz, 2H), 3.71 (t, *J* = 6.0 Hz, 2H), 2.22−2.18 (m, 2H), 1.91 (s, 3H). ESI-MS: *m*/*z* = 384.2 $[M + H]^+$.

*3-Benzyloxy-1-(4-(3-chloropropoxy)phenyl)- pyridin-4(1H)-one (**3d**).* Yellow solid, yield 70%. ^1H NMR (500 MHz, $CDCl_3$): δ

DOI: 10.1021/acschemneuro.5b00224
ACS Chem. Neurosci. 2016, 7, 69−81

7.37−7.35 (m, 3H), 7.31−7.27 (m, 2H), 7.26−7.22 (m, 1H), 7.15 (d, J = 2.0 Hz, 1H), 7.07 (d, J = 9.0 Hz, 2H), 6.91 (d, J = 9.0 Hz, 2H), 6.54 (d, J = 7.5 Hz, 1H), 5.14 (s, 2H), 4.09 (t, J = 6.0 Hz, 2H), 3.71 (t, J = 6.0 Hz, 2H), 2.20−2.17 (m, 2H). ESI-MS: m/z = 370.4 $[M + H]^+$.

*3-Benzyloxy-1-(3-(3-chloropropoxy)phenyl)-2-methylpyridin-4(1H)-one (**3e**).* Yellow solid, yield 86%. ^{1}H NMR (500 MHz, $CDCl_3$): δ 7.38−7.37 (m, 2H), 7.33−7.29 (m, 1H), 7.29−7.23 (m, 3H), 7.22−7.20 (m, 1H), 6.95−6.93 (m, 1H), 6.71−6.68 (m, 1H), 6.65−6.63 (m, 1H), 6.45 (d, J = 7.5 Hz, 1H), 5.20 (s, 2H), 4.07 (t, J = 6.0 Hz, 2H), 3.70 (t, J = 6.0 Hz, 2H), 2.21−2.16 (m, 2H), 1.78 (s, 3H). ESI-MS: m/z = 384.3 $[M + H]^+$.

*3-Benzyloxy-1-(3-(2-bromoethoxy)phenyl)-2-methylpyridin-4(1H)-one (**3f**).* Yellow solid, yield 59%. ^{1}H NMR (500 MHz, $CDCl_3$): δ 7.44−7.42 (m, 2H), 7.35−7.32 (m, 3H), 7.26 (d, J = 7.5 Hz, 1H), 7.12 (d, J = 9.0 Hz, 2H), 7.00 (d, J = 9.0 Hz, 2H), 6.49 (d, J = 7.5 Hz, 1H), 5.25 (s, 2H), 4.34 (t, J = 6.0 Hz, 2H), 3.68 (t, J = 6.0 Hz, 2H), 1.82 (s, 3H). ESI-MS: m/z = 414.3 $[M + H]^+$.

*3-Benzyloxy-1-(3-(4-bromobutoxy)phenyl)-2-methylpyridin-4(1H)-one (**3g**).* Yellow solid, yield 64%. ^{1}H NMR (500 MHz, $CDCl_3$): δ 7.44−7.42 (m, 2H), 7.35−7.32 (m, 3H), 7.26 (d, J = 7.5 Hz, 1H), 7.10 (d, J = 9.0 Hz, 2H), 6.96 (d, J = 9.0 Hz, 2H), 6.55 (d, J = 7.5 Hz, 1H), 5.27 (s, 2H), 4.05 (t, J = 6.0 Hz, 2H), 3.51 (t, J = 6.0 Hz, 2H), 2.09−2.07 (m, 2H), 2.01−1.97 (m, 2H), 1.83 (s, 3H). ESI-MS: m/z = 442.1 $[M + H]^+$.

*3-Benzyloxy-1-(3-((5-bromopentyl)oxy)phenyl)-2-methylpyridin-4(1H)-one (**3h**).* Yellow solid, yield 57%. ^{1}H NMR (500 MHz, $CDCl_3$): δ 7.44−7.42 (m, 2H), 7.35−7.32 (m, 3H), 7.26 (d, J = 7.5 Hz, 1H), 7.09 (d, J = 9.0 Hz, 2H), 6.95 (d, J = 9.0 Hz, 2H), 6.46 (d, J = 7.5 Hz, 1H), 5.27 (s, 2H), 4.02 (t, J = 6.0 Hz, 2H), 3.48−3.44 (m, 2H), 1.99−1.93 (m, 2H), 1.88−1.85 (m, 2H), 1.81 (s, 3H), 1.70−1.64 (m, 2H). ESI-MS: m/z = 456.3 $[M + H]^+$.

General Synthetic Procedure for 4a−p. A mixture of halides **3a−h** (3.6 mmol), secondary amine (11.0 mmol), and triethylamine (2.7 mL, 18 mmol) was refluxed in 20 mL of acetonitrile for 16−24 h. The mixture was cooled to room temperature, filtered, washed with acetonitrile, and concentrated to dryness. The residue was redissolved in ethyl acetate (60 mL), washed with saturated NaCl solution, and dried over anhydrous Na_2SO_4. The solvent was removed under vacuum, and the residue was purified by silica gel chromatography to afford **4a−p**.

*3-Benzyloxy-1-(4-(3-(diethylamino)propoxy)phenyl)-2-methylpyridin-4(1H)-one (**4a**).* Pale-yellow solid, yield 76%. ^{1}H NMR (500 MHz, $CDCl_3$): δ 7.45−7.43 (m, 2H), 7.36−7.31 (m, 3H), 7.26 (d, J = 7.5 Hz, 1H), 7.08 (d, J = 9.0 Hz, 2H), 6.96 (d, J = 9.0 Hz, 2H), 6.47 (d, J = 7.5 Hz, 1H), 5.26 (s, 2H), 4.06 (t, J = 6.0 Hz, 2H), 2.64−2.60 (m, 2H), 2.58 (t, J = 7.5 Hz, 4H), 1.98−1.93 (m, 2H), 1.80 (s, 1H), 1.06 (t, J = 7.5 Hz, 6H). ESI-MS: m/z = 421.4 $[M + H]^+$.

*3-Benzyloxy-1-(4-(3-(dimethylamino)propoxy)phenyl)-2-methylpyridin-4(1H)-one (**4b**).* Pale-yellow solid, yield 69%. ^{1}H NMR (500 MHz, $CDCl_3$): δ 7.44−7.42 (m, 2H), 7.36−7.31 (m, 3H), 7.25 (d, J = 7.5 Hz, 1H), 7.10 (d, J = 9.0 Hz, 2H), 6.97 (d, J = 9.0 Hz, 2H), 6.47 (d, J = 7.5 Hz, 1H), 5.25 (s, 2H), 4.14 (t, J = 6.0 Hz, 2H), 3.04−3.01 (m, 2H), 2.69 (s, 6H), 2.32−2.26 (m, 2H). ESI-MS: m/z = 393.2 $[M + H]^+$.

*3-Benzyloxy-2-methyl-1-(4-(3-(pyrrolidin-1-yl)propoxy)phenyl)-pyridin-4(1H)-one (**4c**).* Pale-yellow solid, yield 82%. ^{1}H NMR (500 MHz, $CDCl_3$): δ 7.38−7.36 (m, 2H), 7.28−7.22 (m, 3H), 7.17 (d, J = 7.5 Hz, 1H), 7.01 (d, J = 9.0 Hz, 2H), 6.89 (d, J = 9.0 Hz, 2H), 6.39 (d, J = 7.5 Hz, 1H), 5.20(s, 2H), 4.06 (t, J = 6.0 Hz, 2H), 2.92−2.82 (m, 6H), 2.19−2.16 (m, 2H), 1.95−1.92 (m, 4H), 1.73 (s, 3H). ESI-MS: m/z = 419.3 $[M + H]^+$.

*3-Benzyloxy-2-methyl-1-(4-(3-(piperidin-1-yl)propoxy)phenyl)-pyridin-4(1H)-one (**4d**).* Pale-yellow solid, yield 74%. ^{1}H NMR (500 MHz, $CDCl_3$): δ 7.38−7.36 (m, 2H), 7.28−7.22 (m, 3H), 7.17 (d, J = 7.5 Hz, 1H), 7.00 (d, J = 9.0 Hz, 2H), 6.89 (d, J = 9.0 Hz, 2H), 6.39 (d, J = 7.5 Hz, 1H), 5.20 (s, 2H), 4.01 (t, J = 6.0 Hz, 2H), 2.64−2.44 (m, 6H), 2.10−2.03 (m, 2H), 1.73 (s, 3H), 1.69−1.64 (m, 4H), 1.48−1.42 (m, 2H). ESI-MS: m/z = 433.4 $[M + H]^+$.

*3-Benzyloxy-2-methyl-1-(4-(3-morpholinopropoxy)phenyl)-pyridin-4(1H)-one (**4e**).* Pale-yellow solid, yield 68%. ^{1}H NMR (500 MHz, $CDCl_3$): δ 7.38−7.36 (m, 2H), 7.28−7.22 (m, 3H), 7.18 (d, J = 7.5 Hz, 1H), 7.02 (d, J = 9.0 Hz, 2H), 6.90 (d, J = 9.0 Hz, 2H), 6.40 (d, J = 7.5 Hz, 1H), 5.21 (s, 2H), 4.01 (t, J = 6.0 Hz, 2H), 3.69−3.65 (m, 4H), 2.49−2.46 (m, 2H), 2.45−2.41 (m, 4H), 1.96−1.93 (m, 2H), 1.75 (s, 3H). ESI-MS: m/z = 435.1 $[M + H]^+$.

*3-Benzyloxy-2-methyl-1-(4-(3-(4-methylpiperazin-1-yl)propoxy)-phenyl)pyridin-4(1H)-one (**4f**).* Pale-yellow solid, yield 73%. ^{1}H NMR (500 MHz, $CDCl_3$): δ 7.45−7.43 (m, 2H), 7.36−7.30 (m, 3H), 7.25 (d, J = 7.5 Hz, 1H), 7.09 (d, J = 9.0 Hz, 2H), 6.95 (d, J = 9.0 Hz, 2H), 6.49 (d, J = 7.5 Hz, 1H), 5.26 (s, 2H), 4.06 (t, J = 6.0 Hz, 2H), 2.94−2.86 (m, 6H), 2.78−2.72 (m, 4H), 2.62 (s, 3H), 2.10−2.05 (m, 2H), 1.81 (s, 3H). ESI-MS: m/z = 448.4 $[M + H]^+$.

*3-Benzyloxy-2-ethyl-1-(4-(3-(diethylamino)propoxy)phenyl)-pyridin-4(1H)-one (**4g**).* Pale-yellow solid, yield 77%. ^{1}H NMR (500 MHz, $CDCl_3$): δ 7.48−7.47 (m, 2H), 7.36−7.34 (m, 2H), 7.31−7.29 (m, 1H), 7.21 (d, J = 7.5 Hz, 1H), 7.15 (d, J = 9.0 Hz, 2H), 6.97 (d, J = 9.0 Hz, 2H), 6.46 (d, J = 7.5 Hz, 1H), 5.32 (s, 2H), 4.07 (t, J = 6.0 Hz, 2H), 2.67−2.64 (m, 2H), 2.61 (q, J = 7.5 Hz, 4H), 2.38 (q, J = 7.5 Hz, 2H), 2.01−1.95 (m, 2H), 1.07 (t, J = 7.5 Hz, 6H), 0.84 (t, J = 7.5 Hz, 3H). ESI-MS: m/z = 435.5 $[M + H]^+$.

*3-Benzyloxy-2-ethyl-1-(4-(3-(pyrrolidin-1-yl)propoxy)phenyl)-pyridin-4(1H)-one (**4h**).* Pale-yellow solid, yield 74%. ^{1}H NMR (500 MHz, $CDCl_3$): δ 7.41−7.39 (m, 2H), 7.29−7.26 (m, 2H), 7.24−7.23 (m, 1H), 7.14 (d, J = 7.5 Hz, 1H), 7.08 (d, J = 9.0 Hz, 2H), 6.90 (d, J = 9.0 Hz, 2H), 6.39 (d, J = 7.5 Hz, 1H), 5.25 (s, 2H), 4.02 (t, J = 6.0 Hz, 2H), 2.61−2.57 (m, 2H), 2.52−2.47 (m, 4H), 2.31 (q, J = 7.5 Hz, 2H), 2.01−1.97 (m, 2H), 1.78−1.73 (m, 4H), 0.77 (t, J = 7.5 Hz, 3H). ESI-MS: m/z = 433.4 $[M + H]^+$.

*5-Benzyloxy-2-methyl-1-(4-(3-(diethylamino)propoxy)phenyl)-pyridin-4(1H)-one (**4i**).* Pale-yellow solid, yield 71%. ^{1}H NMR (500 MHz, $CDCl_3$): δ 7.40−7.38 (m, 2H), 7.35−7.32 (m, 2H), 7.30−7.28 (m, 1H), 7.06 (d, J = 9.0 Hz, 2H), 6.98 (s, 1H), 6.60 (d, J = 9.0 Hz, 2H), 6.40 (s, 1H), 5.13 (s, 2H), 4.07 (t, J = 6.0 Hz, 2H), 2.66 (t, J = 6.0 Hz, 2H), 2.61 (q, J = 7.5 Hz, 4H), 2.00−1.95 (m, 2H), 1.97 (s, 3H), 1.07 (t, J = 7.5 Hz, 4H). ESI-MS: m/z = 421.3 $[M + H]^+$.

*5-Benzyloxy-2-methyl-1-(4-(3-(pyrrolidin-1-yl)propoxy)phenyl)-pyridin-4(1H)-one (**4j**).* Pale-yellow solid, yield 76%. ^{1}H NMR (500 MHz, $CDCl_3$): δ 7.33−7.31 (m, 2H), 7.28−7.26 (m, 2H), 7.26−7.22 (m, 1H), 7.00 (d, J = 9.0 Hz, 2H), 6.91 (s, 1H), 6.89 (d, J = 9.0 Hz, 2H), 6.33 (s, 1H), 5.06 (s, 2H), 4.04 (t, J = 6.0 Hz, 2H), 2.82−2.79 (m, 2H), 2.79−2.73 (m, 4H), 2.14−2.09 (m, 2H), 1.90 (s, 3H), 1.89−1.85 (m, 4H). ESI-MS: m/z = 419.3 $[M + H]^+$.

*3-Benzyloxy-1-(4-(3-(diethylamino)propoxy)phenyl)pyridin-4(1H)-one (**4k**).* Pale-yellow solid, yield 69%. ^{1}H NMR (500 MHz, $CDCl_3$): δ 7.44−7.40 (m, 3H), 7.38−7.35 (m, 2H), 7.32−7.30 (m, 1H), 7.20 (d, J = 2.5 Hz, 1H), 7.12 (d, J = 9.0 Hz, 2H), 6.96 (d, J = 9.0 Hz, 2H), 6.55 (d, J = 7.0 Hz, 1H), 5.21 (s, 2H), 4.05 (t, J = 6.0 Hz, 2H), 2.64 (t, J = 7.0 Hz, 2H), 2.59 (q, J = 7.5 Hz, 4H), 1.99−1.93 (m, 2H), 1.06 (t, J = 7.5 Hz, 6H). ESI-MS: m/z = 407.4 $[M + H]^+$.

*3-Benzyloxy-1-(4-(3-(pyrrolidin-1-yl)propoxy)phenyl)pyridin-4(1H)-one (**4l**).* Pale-yellow solid, yield 78%. ^{1}H NMR (500 MHz, $CDCl_3$): δ 7.37−7.35 (m, 3H), 7.31−7.27 (m, 2H), 7.26−7.22 (m, 1H), 7.15 (d, J = 2.0 Hz, 1H), 7.06 (d, J = 9.0 Hz, 2H), 6.89 (d, J = 9.0 Hz, 2H), 6.48 (d, J = 7.5 Hz, 1H), 5.14 (s, 2H), 4.04 (t, J = 6.0 Hz, 2H), 2.83−2.80 (m, 2H), 2.78−2.72 (m, 4H), 2.13−2.10 (m, 2H), 1.91−1.86 (m, 4H). ESI-MS: m/z = 405.3 $[M + H]^+$.

*3-Benzyloxy-2-methyl-1-(3-(3-(pyrrolidin-1-yl)propoxy)phenyl)-pyridin-4(1H)-one (**4m**).* Pale-yellow solid, yield 72%. ^{1}H NMR (500 MHz, $CDCl_3$): δ 7.45−7.43 (m, 2H), 7.37−7.30 (m, 4H), 7.27−7.24 (m, 2H), 7.00−6.98 (m, 1H), 6.74−6.72 (m, 1H), 6.69 (s, 1H), 6.47 (d, J = 7.5 Hz, 1H), 5.27 (s, 2H), 4.06 (t, J = 6.0 Hz, 2H), 2.69−2.66 (m, 2H), 2.62−2.57 (m, 4H), 2.06−2.03 (m, 2H), 1.85 (s, 3H), 1.80−1.78 (m, 4H). ESI-MS: m/z = 419.2 $[M + H]^+$.

*3-Benzyloxy-2-methyl-1-(4-(2-(pyrrolidin-1-yl)ethoxy)phenyl)-pyridin-4(1H)-one (**4n**).* Pale-yellow solid, yield 68%. ^{1}H NMR (500 MHz, $CDCl_3$): δ 7.44−7.42 (m, 2H), 7.35−7.30 (m, 3H), 7.26 (d, J = 7.5 Hz, 1H), 7.08 (d, J = 9.0 Hz, 2H), 6.99 (d, J = 9.0 Hz, 2H), 6.48 (d, J = 7.5 Hz, 1H), 5.25 (s, 2H), 4.16 (t, J = 6.0 Hz, 2H), 2.96 (t, J = 6.0 Hz, 2H), 2.67−2.64 (m, 4H), 1.84−1.82 (m, 4H), 1.81 (s, 3H). ESI-MS: m/z = 405.3 $[M + H]^+$.

*3-Benzyloxy-2-methyl-1-(4-(4-(pyrrolidin-1-yl)butoxy)phenyl)-pyridin-4(1H)-one (**4o**).* Pale-yellow solid, yield 73%. ^{1}H NMR (500

DOI: 10.1021/acschemneuro.5b00224
ACS Chem. Neurosci. 2016, 7, 69−81

MHz, $CDCl_3$): δ 7.44−7.42 (m, 2H), 7.35−7.30 (m, 3H), 7.26 (d, *J* = 7.5 Hz, 1H), 7.08 (d, *J* = 9.0 Hz, 2H), 6.95 (d, *J* = 9.0 Hz, 2H), 6.47 (d, *J* = 7.5 Hz, 1H), 5.25 (s, 2H), 4.03 (t, *J* = 6.0 Hz, 2H), 2.55−2.52 (m, 6H), 1.88−1.83 (m, 2H), 1.81 (s, 3H), 1.80−1.75 (m, 4H), 1.73−1.69 (m, 2H). ESI-MS: *m*/*z* = 433.4 $[M + H]^+$.

3-Benzyloxy-2-methyl-1-(4-((5-(pyrrolidin-1-yl)pentyl)oxy)-phenyl)pyridin-4(1H)-one (***4p***). Pale-yellow solid, yield 65%. ^1H NMR (500 MHz, $CDCl_3$): δ 7.44−7.42 (m, 2H), 7.35−7.30 (m, 3H), 7.26 (d, *J* = 7.5 Hz, 1H), 7.07 (d, *J* = 9.0 Hz, 2H), 6.95 (d, *J* = 9.0 Hz, 2H), 6.46 (d, *J* = 7.5 Hz, 1H), 5.25 (s, 2H), 4.00 (t, *J* = 6.0 Hz, 2H), 2.54−2.50 (m, 4H), 2.48−2.46 (m, 2H), 1.86−1.82 (m, 2H), 1.81 (s, 3H), 1.80−1.77 (m, 4H), 1.64−1.58 (m, 2H), 1.55−1.49 (m, 2H). ESI-MS: *m*/*z* = 447.3 $[M + H]^+$.

General Synthetic Procedure for 5a−g. A mixture of compounds **4a−g** (1.2 mmol), 10% Pd/C (10% weight of **4a−g**), and 10 mL of methanol was stirred overnight under hydrogen atmosphere. After the catalyst was filtered off, the filtrate was concentrated to yield crude product, which was purified by silica gel chromatography to give **5a−g**.

3-Hydroxy-2-methyl-1-(4-(3-(diethylamino)propoxy)phenyl)-pyridin-4(1H)-one (***5a***). White solid, yield 93%. Mp 229−232 °C. ^1H NMR (500 MHz, $CDCl_3$): δ 7.30 (d, *J* = 7.5 Hz, 1H), 7.18 (d, *J* = 9.0 Hz, 2H), 7.00 (d, *J* = 9.0 Hz, 2H), 6.47 (d, *J* = 7.5 Hz, 1H), 4.10 (t, *J* = 6.5 Hz, 2H), 2.87 (t, *J* = 7.5 Hz, 2H), 2.80 (q, *J* = 7.5 Hz, 4H), 2.12−2.06 (m, 2H), 2.10 (s, 3H), 1.17 (t, *J* = 7.5 Hz, 6H). ^{13}C NMR (125 MHz, $CDCl_3$): δ 170.02, 159.36, 145.62, 137.73, 134.62, 129.39, 127.84, 115.34, 110.94, 66.41, 48.83, 46.30, 25.60, 13.61, 10.31. HRMS (ESI) (*m*/*z*): calcd for $C_{19}H_{27}N_2O_3$ $[M + H]^+$ 331.2022, found 331.2020. HPLC purity: 96.8%, R_t 6.07 min.

3-Hydroxy-2-methyl-1-(4-(3-(dimethylamino)propoxy)phenyl)-pyridin-4(1H)-one (***5b***). White solid, yield 95%. ^1H NMR (500 MHz, $CDCl_3$): δ 7.29 (d, *J* = 7.5 Hz, 1H), 7.18 (d, *J* = 9.0 Hz, 2H), 7.01 (d, *J* = 9.0 Hz, 2H), 6.46 (d, *J* = 7.5 Hz, 1H), 4.12 (t, *J* = 6.5 Hz, 2H), 2.73 (t, *J* = 7.5 Hz, 2H), 2.44 (s, 6H), 2.14−2.11 (m, 2H), 2.10 (s, 3H). ^{13}C NMR (125 MHz, $CDCl_3$): δ 170.05, 159.35, 145.59, 137.76, 134.64, 129.20, 127.85, 115.35, 110.87, 66.26, 55.89, 44.70, 26.51, 13.61. HRMS (ESI) (*m*/*z*): calcd for $C_{17}H_{23}N_2O_3$ $[M + H]^+$ 303.1709, found 303.1708. HPLC purity: 95.2%, R_t 5.25 min.

3-Hydroxy-2-methyl-1-(4-(3-(pyrrolidin-1-yl)propoxy)phenyl)-pyridin-4(1H)-one (***5c***). White solid, yield 96%. Mp 205−207 °C. ^1H NMR (500 MHz, $CDCl_3$): δ 7.30 (d, *J* = 7.5 Hz, 1H), 7.18 (d, *J* = 9.0 Hz, 2H), 7.02 (d, *J* = 9.0 Hz, 2H), 6.46 (d, *J* = 7.5 Hz, 1H), 4.13 (t, *J* = 6.5 Hz, 2H), 2.71 (t, *J* = 7.5 Hz, 2H), 2.64−2.56 (m, 4H), 2.10−2.05 (m, 2H), 2.07 (s, 3H), 1.88−1.84 (m, 4H). ^{13}C NMR (125 MHz, $CDCl_3$): δ 170.09, 159.21, 145.56, 137.78, 134.75, 128.94, 127.91, 115.37, 110.78, 66.15, 54.11, 53.01, 27.37, 23.46, 13.59. HRMS (ESI) (*m*/*z*): calcd for $C_{19}H_{25}N_2O_3$ $[M + H]^+$ 329.1865, found 329.1861. HPLC purity: 98.3%, R_t 5.97 min.

3-Hydroxy-2-methyl-1-(4-(3-(piperidin-1-yl)propoxy)phenyl)-pyridin-4(1H)-one (***5d***). White solid, yield 96%. Mp 182−185 °C. ^1H NMR (500 MHz, $CDCl_3$): δ 7.29 (d, *J* = 7.0 Hz, 1H), 7.18 (d, *J* = 9.0 Hz, 2H), 7.00 (d, *J* = 9.0 Hz, 2H), 6.45 (d, *J* = 7.0 Hz, 1H), 4.12 (t, *J* = 6.0 Hz, 2H), 2.80 (t, *J* = 7.5 Hz, 2H), 2.76−2.68 (m, 4H), 2.26-2.18(m, 2H), 2.09 (s, 3H), 1.84−1.78(m, 4H), 1.60−1.53 (m, 2H). ^{13}C NMR (125 MHz, $CDCl_3$): δ 170.09, 159.28, 145.57, 137.80, 134.72, 128.97, 127.90, 115.38, 110.78, 66.43, 55.56, 54.26, 25.57, 24.60, 23.48, 13.59. HRMS (ESI) (*m*/*z*): calcd for $C_{20}H_{27}N_2O_3$ $[M + H]^+$ 343.2022, found 343.2020. HPLC purity: 97.6%, R_t 6.39 min.

3-Hydroxy-2-methyl-1-(4-(3-morpholinopropoxy)phenyl)pyridin-4(1H)-one (***5e***). White solid, yield 95%. Mp 196−199 °C. ^1H NMR (500 MHz, $CDCl_3$): δ 7.29 (d, *J* = 7.0 Hz, 1H), 7.18 (d, *J* = 9.0 Hz, 2H), 7.01 (d, *J* = 9.0 Hz, 2H), 6.45 (d, *J* = 7.0 Hz, 1H), 4.10 (t, *J* = 6.0 Hz, 2H), 3.76−3.74 (m, 4H), 2.59−2.56 (m, 2H), 2.54−2.48 (m, 4H), 2.10 (s, 3H), 2.06−2.00 (m, 2H). ^{13}C NMR (125 MHz, $CDCl_3$): δ 170.08, 159.49, 145.57, 137.78, 134.53, 128.98, 127.86, 115.31, 110.80, 66.89, 66.53, 55.42, 53.72, 26.24, 13.62. HRMS (ESI) (*m*/*z*): calcd for $C_{19}H_{25}N_2O_4$ $[M + H]^+$ 345.1814, found 345.1816. HPLC purity: 97.1%, R_t 5.45 min.

3-Hydroxy-2-methyl-1-(4-(3-(4-methylpiperazin-1-yl)propoxy)-phenyl)pyridin-4(1H)-one (***5f***). White solid, yield 98%. Mp 138−140 °C. ^1H NMR (400 MHz, $CDCl_3$): δ 7.29 (d, *J* = 7.2 Hz, 1H), 7.17 (d, *J* = 8.8 Hz, 2H), 7.00 (d, *J* = 8.8 Hz, 2H), 6.45 (d, *J* = 7.2 Hz, 1H), 4.09 (t, *J* = 6.0 Hz, 2H), 2.61−2.50 (m, 10H), 2.34 (s, 3H), 2.09 (s, 3H), 2.06−1.99 (m, 2H). ^{13}C NMR (100 MHz, $CDCl_3$): δ 170.07, 159.53, 145.54, 137.82, 134.51, 128.86, 127.84, 115.34, 110.71, 66.66, 54.96, 54.91, 52.94, 45.85, 38.66, 26.59, 13.59. HRMS (ESI) (*m*/*z*): calcd for $C_{20}H_{28}N_3O_3$ $[M + H]^+$ 358.2125, found 358.2130. HPLC purity: 98.8%, R_t 5.33 min.

2-Ethyl-3-hydroxy-1-(4-(3-(diethylamino)propoxy)phenyl)-pyridin-4(1H)-one (***5g***). White solid, yield 96%. Mp 137−140 °C. ^1H NMR (500 MHz, $CDCl_3$): δ 7.24 (d, *J* = 6.0 Hz, 1H), 7.20 (d, *J* = 7.2 Hz, 2H), 6.99 (d, *J* = 7.2 Hz, 2H), 6.43 (d, *J* = 6.0 Hz, 1H), 4.10 (t, *J* = 5.2 Hz, 2H), 2.67−2.65 (m, 2H), 2.61 (q, *J* = 5.2 Hz, 4H), 2.55 (q, *J* = 6.0 Hz, 2H), 2.02−1.97 (m, 2H), 1.08 (t, *J* = 5.2 Hz, 6H), 1.08 (t, *J* = 6.0 Hz, 3H). ^{13}C NMR (125 MHz, $CDCl_3$): δ 170.26, 159.55, 145.19, 137.98, 134.73, 134.29, 128.08, 115.18, 110.81, 66.64, 49.02, 46.62, 26.27, 20.38, 12.39, 11.02. HRMS (ESI) (*m*/*z*): calcd for $C_{20}H_{29}N_2O_3$ $[M + H]^+$ 345.2173, found 345.2181. HPLC purity: 98.5%, R_t 6.92 min.

2-Ethyl-3-hydroxy-1-(4-(3-(pyrrolidin-1-yl)propoxy)phenyl)-pyridin-4(1H)-one (***5h***). White solid, yield 99%. Mp 189−191 °C. ^1H NMR (500 MHz, $CDCl_3$): δ 7.21 (d, *J* = 7.0 Hz, 1H), 7.19 (d, *J* = 9.0 Hz, 2H), 6.99 (d, *J* = 9.0 Hz, 2H), 6.43 (d, *J* = 7.0 Hz, 1H), 4.10 (t, *J* = 6.0 Hz, 2H), 2.69 (t, *J* = 7.5 Hz, 2H), 2.61−2.55 (m, 4H), 2.54 (q, *J* = 7.5 Hz, 2H), 2.10−2.02 (m, 2H), 1.84−1.78 (m, 4H), 1.01 (t, *J* = 7.5 Hz, 3H). ^{13}C NMR (125 MHz, $CDCl_3$): δ 170.29, 159.60, 145.18, 138.00, 134.48, 134.28, 128.07, 115.22, 110.70, 66.80, 54.26, 52.99, 28.57, 23.48, 20.37, 12.40. HRMS (ESI) (*m*/*z*): calcd for $C_{20}H_{27}N_2O_3$ $[M + H]^+$ 343.2022, found 343.2033. HPLC purity: 97.2%, R_t 6.78 min.

5-Hydroxy-2-methyl-1-(4-(3-(diethylamino)propoxy)phenyl)-pyridin-4(1H)-one (***5i***). White solid, yield 97%. Mp >250 °C. ^1H NMR (400 MHz, $CDCl_3$): δ 7.22 (s, 1H), 7.17 (d, *J* = 8.8 Hz, 2H), 7.00 (d, *J* = 8.8 Hz, 2H), 6.40 (s, 1H), 4.09 (t, *J* = 6.0 Hz, 2H), 2.67−2.63 (m, 2H), 2.61 (q, *J* = 7.2 Hz, 2H), 2.04 (s, 3H), 2.02−1.95 (m, 2H), 1.07 (t, *J* = 7.2 Hz, 2H). ^{13}C NMR (125 MHz, $CDCl_3$): δ 171.60, 159.49, 146.41, 145.76, 134.72, 127.69, 122.65, 115.40, 113.10, 66.65, 49.04, 46.66, 26.33, 20.39, 11.10. HRMS (ESI) (*m*/*z*): calcd for $C_{19}H_{27}N_2O_3$ $[M + H]^+$ 331.2016, found 331.2022. HPLC purity: 96.0%, R_t 5.69 min.

5-Hydroxy-2-methyl-1-(4-(3-(pyrrolidin-1-yl)propoxy)phenyl)-pyridin-4(1H)-one (***5j***). White solid, yield 98%. Mp 196−199 °C.^1H NMR (500 MHz, $CDCl_3$): δ 7.28 (s, 1H), 7.17 (d, *J* = 9.0 Hz, 2H), 7.00 (d, *J* = 9.0 Hz, 2H), 6.40 (s, 1H), 4.17−4.13 (m, 2H), 3.02−2.96 (m, 6H), 2.26−2.23(m, 2H), 2.03 (s, 3H), 2.01−1.98 (m, 4H). ^{13}C NMR (125 MHz, $CDCl_3$): δ 171.65, 159.20, 146.33, 145.77, 134.85, 127.72, 122.99, 115.47, 113.31, 66.07, 53.98, 52.88, 27.13, 23.40, 20.35. HRMS (ESI) (*m*/*z*): calcd for $C_{19}H_{25}N_2O_3$ $[M + H]^+$ 329.1865, found 329.1864. HPLC purity: 98.5%, R_t 5.28 min.

3-Hydroxy-1-(4-(3-(diethylamino)propoxy)phenyl)pyridin-4(1H)-one (***5k***). White solid, yield 95%. Mp 191−193 °C. ^1H NMR (500 MHz, $CDCl_3$): δ 7.49−7.47 (m, 2H), 7.27 (d, *J* = 9.0 Hz, 2H), 7.00 (d, *J* = 9.0 Hz, 2H), 6.55 (d, *J* = 7.0 Hz, 1H), 4.08 (t, *J* = 6.0 Hz, 2H), 2.78−2.75 (m, 2H), 2.72 (q, *J* = 7.0 Hz, 4H), 2.05−2.02 (m, 2H), 1.12 (t, *J* = 7.0 Hz, 6H). ^{13}C NMR (125 MHz, $CDCl_3$): δ 171.14, 158.94, 148.31, 136.76, 136.36, 124.34, 120.87, 115.63, 112.81, 66.58, 48.95, 46.54, 26.07, 10.83. HRMS (ESI) (*m*/*z*): calcd for $C_{18}H_{25}N_2O_3$ $[M + H]^+$ 317.1860, found 317.1866. HPLC purity: 99.0%, R_t 5.70 min.

3-Hydroxy-1-(4-(3-(pyrrolidin-1-yl)propoxy)phenyl)pyridin-4(1H)-one (***5l***). White solid, yield 99%. Mp 185−188 °C. ^1H NMR (500 MHz, $CDCl_3$): δ 7.50−7.45 (m, 2H), 7.28 (d, *J* = 9.0 Hz, 2H), 7.00 (d, *J* = 9.0 Hz, 2H), 6.55 (d, *J* = 7.0 Hz, 1H), 4.14 (t, *J* = 6.0 Hz, 2H), 3.00−2.92 (m, 6H), 2.28−2.22 (m, 2H), 2.03−1.97 (m, 4H). ^{13}C NMR (125 MHz, $CDCl_3$): δ 171.02, 158.70, 148.08, 137.03, 136.54, 124.44, 120.37, 115.70, 112.57, 66.10, 54.02, 52.96, 27.17, 23.45. HRMS (ESI) (*m*/*z*): calcd for $C_{18}H_{23}N_2O_3$ $[M + H]^+$ 315.1709, found 315.1712. HPLC purity: 99.1%, R_t 5.43 min.

3-Hydroxy-2-methyl-1-(3-(3-(pyrrolidin-1-yl)propoxy)phenyl)-pyridin-4(1H)-one (***5m***). White solid, yield 98%.^1H NMR (500 MHz, $CDCl_3$): δ 7.42 (t, *J* = 8.0 Hz, 1H), 7.31 (d, *J* = 7.5 Hz, 1H), 7.05 (dd,

DOI: 10.1021/acschemneuro.5b00224
ACS Chem. Neurosci. 2016, 7, 69−81

J = 8.5 Hz, 2.0 Hz, 1H), 6.84 (dd, J = 8.5 Hz, 2.0 Hz, 1H), 6.79 (m, 1H), 6.46 (d, J = 7.5 Hz, 1H), 4.08 (t, J = 6.5 Hz, 2H), 2.71 (d, J = 7.5 Hz, 2H), 2.65−2.58 (m, 4H), 2.13 (s, 3H), 2.10−2.04 (m, 2H), 1.85−1.81 (m, 4H). ^{13}C NMR (125 MHz, $CDCl_3$): δ 170.13, 159.97, 145.60, 142.65, 137.33, 130.56, 128.44, 118.77, 115.60, 113.24, 110.79, 66.77, 54.19, 52.92, 28.39, 23.45, 13.54. HRMS (ESI) (m/z): calcd for $C_{19}H_{25}N_2O_3$ $[M + H]^+$ 329.1865, found 329.1867. HPLC purity: 97.9%, R_t 6.46 min.

*3-Hydroxy-2-methyl-1-(4-(2-(pyrrolidin-1-yl)ethoxy)phenyl)-pyridin-4(1H)-one (**5n**)*. White solid, yield 95%. Mp 165−168 °C. ^{1}H NMR (400 MHz, $CDCl_3$): δ 7.30 (d, J = 7.6 Hz, 1H), 7.18 (d, J = 8.8 Hz, 2H), 7.03 (d, J = 8.8 Hz, 2H), 6.46 (d, J = 7.6 Hz, 1H), 4.22 (t, J = 5.6 Hz, 2H), 3.03−2.98 (m, 2H), 2.77−2.68 (m, 4H), 2.10 (s, 3H), 1.90−1.84 (s, 4H). ^{13}C NMR (100 MHz, $CDCl_3$): δ 170.04, 159.24, 145.51, 137.81, 134.66, 128.91, 127.86, 115.42, 110.72, 67.23, 54.83, 54.75, 23.45, 13.61. HRMS (ESI) (m/z): calcd for $C_{18}H_{23}N_2O_3$ $[M + H]^+$ 315.1703, found 315.1708. HPLC purity: 98.1%, R_t 5.04 min.

*3-Hydroxy-2-methyl-1-(4-(4-(pyrrolidin-1-yl)butoxy)phenyl)-pyridin-4(1H)-one (**5o**)*. White solid, yield 97%. Mp 178−181 °C. ^{1}H NMR (400 MHz, $CDCl_3$) δ 7.29 (d, J = 7.6 Hz, 1H), 7.17 (d, J = 8.8 Hz, 2H), 6.99 (d, J = 8.8 Hz, 2H), 6.45 (d, J = 7.6 Hz, 1H), 4.06 (t, J = 6.0 Hz, 2H), 2.73−2.69 (m, 4H), 2.69−2.65 (m, 2H), 2.10 (s, 3H), 1.90−1.87 (m, 6H), 1.81−1.79 (m, 2H). ^{13}C NMR (125 MHz, $CDCl_3$): δ 176.84, 170.00, 159.35, 145.61, 137.72, 134.55, 127.81, 115.34, 110.98, 67.68, 55.20, 53.42, 26.75, 23.58, 23.32, 13.61. HRMS (ESI) (m/z): calcd for $C_{20}H_{27}N_2O_3$ $[M + H]^+$ 343.2016, found 343.2023. HPLC purity: 98.5%, R_t 6.57 min.

*3-Hydroxy-2-methyl-1-(4-((5-(pyrrolidin-1-yl)pentyl)oxy)phenyl)-pyridin-4(1H)-one (**5p**)*. White solid, yield 95%. Mp 186−189 °C. ^{1}H NMR (400 MHz, $CDCl_3$) δ 7.29 (d, J = 7.6 Hz, 1H), 7.17 (d, J = 8.8 Hz, 2H), 6.99 (d, J = 8.8 Hz, 2H), 6.45 (d, J = 7.6 Hz, 1H), 4.03 (t, J = 6.0 Hz, 2H), 2.71−2.66 (m, 4H), 2.66−2.60 (m, 2H), 2.09 (s, 3H), 1.88−1.83 (m, 6H), 1.72−1.68 (m, 2H), 1.58−1.52 (m, 2H). ^{13}C NMR (125 MHz, $CDCl_3$): δ 170.06, 159.58, 145.56, 137.80, 134.46, 129.05, 127.81, 115.32, 110.75, 68.13, 56.12, 54.03, 28.89, 27.72, 23.94, 23.38, 13.58. HRMS (ESI) (m/z): calcd for $C_{21}H_{29}N_2O_3$ $[M + H]^+$ 357.2173, found 357.2179. HPLC purity: 97.8%, R_t 7.39 min.

■ ASSOCIATED CONTENT

Supporting Information

The Supporting Information is available free of charge on the ACS Publications website at DOI: 10.1021/acschemneuro.5b00224.

Experimental procedures for the druglikeness evaluation and log BB calculation, LANCE TR-FRET assay, CRE-driven luciferase assay, Aβ peptide and metal chelating experiments, Trolox-equivalent antioxidant capacity (TEAC) assay, cell viability studies, molecular docking, and determination of plasma and brain drug concentrations and supplementary tables and figures for the physicochemical properties of **5a−p**, Aβ and metal chelating experiments, and time−concentration curve of **5c**. (PDF)

■ AUTHOR INFORMATION

Corresponding Authors

*Rong Sheng. Tel/Fax: +86-571-8820-8458. E-mail address: shengr@zju.edu.cn.

*Yongzhou Hu. Tel/Fax: +86-571-8820-8460. E-mail address: huyz@zju.edu.cn.

Author Contributions

#R.S. and L.T. contributed equally to this work.

Funding

The authors thank the National Natural Science Foundation of China (Grant No. 21172193) and the Zhejiang Provincial Natural Science Foundation of China (Grant No. R2110297) for financial support.

Notes

The authors declare no competing financial interest.

■ ACKNOWLEDGMENTS

We thank Jianyang Pan (Pharmaceutical Informatics Institute, Zhejiang University) for performing NMR and MS for structure elucidation.

■ ABBREVIATIONS USED

ABTS$^{\bullet+}$, 2,2′-azino-bis(3-ethyl-benzothiazoline-6-sulfonic acid) radical cation; Aβ, β-amyloid; AChE, acetylcholinesterase; AD, Alzheimer's disease; BBB, blood−brain barrier; CRE, cAMP-response elements; CQ, clioquinol; EtOH, ethanol; hERG, human ether-à-go-go-related gene; HPLC, high performance liquid chromatography; H_1R, histamine H_1 receptor; H_2R, histamine H_2 receptor; H_3R, histamine H_3 receptor; H_4R, histamine H_4 receptor; K_2CO_3, potassium carbonate; MTDL, multitarget-directed ligands; PK, pharmacokinetic; ROS, reactive oxygen species; SAR, structure−activity relationship; SD, Sprague−Dawley; SRB, sulforhodamine B; TEAC, Trolox-equivalent antioxidant capacity; TEM, transmission electron microscopy; ThT, thioflavin T; TR-FRET, time-resolved fluorescence resonance energy transfer

■ REFERENCES

(1) Finder, V. H. (2010) Alzheimer's disease: a general introduction and pathomechanism. *J. Alzheimers. Dis. 22* (Suppl 3), 5−19.

(2) Sosa-Ortiz, A. L., Acosta-Castillo, I., and Prince, M. J. (2012) Epidemiology of Dementias and Alzheimer's Disease. *Arch. Med. Res. 43* (8), 600−608.

(3) Reitz, C., Brayne, C., and Mayeux, R. (2011) Epidemiology of Alzheimer disease. *Nat. Rev. Neurol. 7* (3), 137−152.

(4) Alzheimer's Association (2013) 2013 Alzheimer's disease facts and figures. *Alzheimer's Dementia 9* (2), 208−245.

(5) Ballard, C., Gauthier, S., Corbett, A., Brayne, C., Aarsland, D., and Jones, E. (2011) Alzheimer's disease. *Lancet 377* (9770), 1019−1031.

(6) Grill, J. D., and Cummings, J. L. (2010) Current therapeutic targets for the treatment of Alzheimer's disease. *Expert Rev. Neurother. 10* (5), 711−728.

(7) Anand, R., Gill, K. D., and Mahdi, A. A. (2014) Therapeutics of Alzheimer's disease: Past, present and future. *Neuropharmacology 76* (Part A), 27−50.

(8) Chiang, K., and Koo, E. H. (2014) Emerging therapeutics for Alzheimer's disease. *Annu. Rev. Pharmacol. Toxicol. 54*, 381−405.

(9) Francis, P. T., Palmer, A. M., Snape, M., and Wilcock, G. K. (1999) The cholinergic hypothesis of Alzheimer's disease: a review of progress. *J. Neurol., Neurosurg. Psychiatry 66* (2), 137−147.

(10) Takeda, A., Loveman, E., Clegg, A., Kirby, J., Picot, J., Payne, E., and Green, C. (2006) A systematic review of the clinical effectiveness of donepezil, rivastigmine and galantamine on cognition, quality of life and adverse events in Alzheimer's disease. *Int. J. Geriatr. Psychiatry. 21* (1), 17−28.

(11) Raina, P., Santaguida, P., Ismaila, A., Patterson, C., Cowan, D., Levine, M., Booker, L., and Oremus, M. (2008) Effectiveness of cholinesterase inhibitors and memantine for treating dementia: Evidence review for a clinical practice guideline. *Ann. Intern. Med. 148* (5), 379−397.

(12) Leon, R., Garcia, A. G., and Marco-Contelles, J. (2013) Recent advances in the multitarget-directed ligands approach for the treatment of Alzheimer's disease. *Med. Res. Rev. 33* (1), 139−189.

(13) Bajda, M., Guzior, N., Ignasik, M., and Malawska, B. (2011) Multi-target-directed ligands in Alzheimer's disease treatment. *Curr. Med. Chem. 18* (32), 4949−4975.

DOI: 10.1021/acschemneuro.5b00224
ACS Chem. Neurosci. 2016, 7, 69−81

(14) Tiligada, E., Kyriakidis, K., Chazot, P. L., and Passani, M. B. (2011) Histamine pharmacology and new CNS drug targets. *CNS Neurosci. Ther. 17* (6), 620−628.
(15) Leurs, R., Bakker, R. A., Timmerman, H., and de Esch, I. J. (2005) The histamine H3 receptor: from gene cloning to H3 receptor drugs. *Nat. Rev. Drug Discovery 4* (2), 107−120.
(16) Berlin, M., Boyce, C. W., and de Lera Ruiz, M. (2011) Histamine H3 receptor as a drug discovery target. *J. Med. Chem. 54* (1), 26−53.
(17) Bhowmik, M., Khanam, R., and Vohora, D. (2012) Histamine H3 receptor antagonists in relation to epilepsy and neurodegeneration: a systemic consideration of recent progress and perspectives. *Br. J. Pharmacol. 167* (7), 1398−1414.
(18) NCT01018875, NCT01548287, NCT01903824, NCT01009255, NCT00675090, NCT00420420, NCT00874939. http://www.clinicaltrials.gov (accessed June 1, 2015).
(19) Hardy, J., and Selkoe, D. J. (2002) The amyloid hypothesis of Alzheimer's disease: progress and problems on the road to therapeutics. *Science 297* (5580), 353−356.
(20) Kung, H. F. (2012) The beta-Amyloid Hypothesis in Alzheimer's Disease: Seeing Is Believing. *ACS Med. Chem. Lett. 3* (4), 265−267.
(21) Hamley, I. W. (2012) The amyloid beta peptide: a chemist's perspective. Role in Alzheimer's and fibrillization. *Chem. Rev. 112* (10), 5147−5192.
(22) Gilbert, B. J. (2013) The role of amyloid beta in the pathogenesis of Alzheimer's disease. *J. Clin. Pathol. 66* (5), 362−366.
(23) Belluti, F., Rampa, A., Gobbi, S., and Bisi, A. (2013) Small-molecule inhibitors/modulators of amyloid-beta peptide aggregation and toxicity for the treatment of Alzheimer's disease: a patent review (2010 - 2012). *Expert Opin. Ther. Pat. 23* (5), 581−596.
(24) Jakob-Roetne, R., and Jacobsen, H. (2009) Alzheimer's disease: from pathology to therapeutic approaches. *Angew. Chem., Int. Ed. 48* (17), 3030−3059.
(25) Duce, J. A., and Bush, A. I. (2010) Biological metals and Alzheimer's disease: implications for therapeutics and diagnostics. *Prog. Neurobiol. 92* (1), 1−18.
(26) Scott, L. E., and Orvig, C. (2009) Medicinal inorganic chemistry approaches to passivation and removal of aberrant metal ions in disease. *Chem. Rev. 109* (10), 4885−4910.
(27) Huang, X., Atwood, C. S., Hartshorn, M. A., Multhaup, G., Goldstein, L. E., Scarpa, R. C., Cuajungco, M. P., Gray, D. N., Lim, J., Moir, R. D., Tanzi, R. E., and Bush, A. I. (1999) The A beta peptide of Alzheimer's disease directly produces hydrogen peroxide through metal ion reduction. *Biochemistry 38* (24), 7609−7616.
(28) Ritchie, C. W., Bush, A. I., Mackinnon, A., Macfarlane, S., Mastwyk, M., MacGregor, L., Kiers, L., Cherny, R., Li, Q., Tammer, A., Carrington, D., Mavros, C., Volitakis, I., Xilinas, M., Ames, D., Davis, S., Beyreuther, K., Tanzi, R. E., and Masters, C. L. (2003) Metal-Protein Attenuation With Iodochlorhydroxyquin (Clioquinol) Targeting Aβ Amyloid Deposition and Toxicity in Alzheimer Disease. *Arch. Neurol. 60* (12), 1685−1691.
(29) NCT00471211. http://www.clinicaltrials.gov (accessed June 1, 2015).
(30) Tang, L., Zhao, L., Hong, L., Yang, F., Sheng, R., Chen, J., Shi, Y., Zhou, N., and Hu, Y. (2013) Design and synthesis of novel 3-substituted-indole derivatives as selective H3 receptor antagonists and potent free radical scavengers. *Bioorg. Med. Chem. 21* (19), 5936−5944.
(31) Łażewska, D., and Kiec-Kononowicz, K. (2014) New developments around histamine H_3 receptor antagonists/inverse agonists: a patent review (2010 - present). *Expert Opin. Ther. Pat. 24* (1), 89−111.
(32) Nagase, T., Mizutani, T., Ishikawa, S., Sekino, E., Sasaki, T., Fujimura, T., Ito, S., Mitobe, Y., Miyamoto, Y., Yoshimoto, R., Tanaka, T., Ishihara, A., Takenaga, N., Tokita, S., Fukami, T., and Sato, N. (2008) Synthesis, structure-activity relationships, and biological profiles of a quinazolinone class of histamine H_3 receptor inverse agonists. *J. Med. Chem. 51* (15), 4780−4789.
(33) Feng, M. H., van der Does, L., and Bantjes, A. (1993) Iron (III)-chelating resins. 3. Synthesis, iron (III)-chelating properties, and in vitro antibacterial activity of compounds containing 3-hydroxy-2-methyl-4(1H)-pyridinone ligands. *J. Med. Chem. 36* (19), 2822−2827.
(34) Scott, L. E., Page, B. D., Patrick, B. O., and Orvig, C. (2008) Altering pyridinone N-substituents to optimize activity as potential prodrugs for Alzheimer's disease. *Dalton Trans. 45*, 6364−6367.
(35) Green, D. E., Bowen, M. L., Scott, L. E., Storr, T., Merkel, M., Bohmerle, K., Thompson, K. H., Patrick, B. O., Schugar, H. J., and Orvig, C. (2010) In vitro studies of 3-hydroxy-4-pyridinones and their glycosylated derivatives as potential agents for Alzheimer's disease. *Dalton Trans. 39* (6), 1604−1615.
(36) Howlett, D. R., Perry, A. E., Godfrey, F., Swatton, J. E., Jennings, K. H., Spitzfaden, C., Wadsworth, H., Wood, S. J., and Markwell, R. E. (1999) Inhibition of fibril formation in beta-amyloid peptide by a novel series of benzofurans. *Biochem. J. 340*, 283−289.
(37) Shimamura, T., Shiroishi, M., Weyand, S., Tsujimoto, H., Winter, G., Katritch, V., Abagyan, R., Cherezov, V., Liu, W., Han, G. W., Kobayashi, T., Stevens, R. C., and Iwata, S. (2011) Structure of the human histamine H1 receptor complex with doxepin. *Nature 475* (7354), 65−70.
(38) Crescenzi, O., Tomaselli, S., Guerrini, R., Salvadori, S., D'Ursi, A. M., Temussi, P. A., and Picone, D. (2002) Solution structure of the Alzheimer amyloid beta-peptide (1−42) in an apolar microenvironment. Similarity with a virus fusion domain. *Eur. J. Biochem. 269* (22), 5642−5648.
(39) Kim, S., Fristrup, P., Abrol, R., and Goddard, W. A. (2011) Structure-based prediction of subtype selectivity of histamine H_3 receptor selective antagonists in clinical trials. *J. Chem. Inf. Model. 51*, 3262−3274.
(40) Lu, C., Guo, Y., Yan, J., Luo, Z., Luo, H. B., Yan, M., Huang, L., and Li, X. (2013) Design, synthesis, and evaluation of multitarget-directed resveratrol derivatives for the treatment of Alzheimer's disease. *J. Med. Chem. 56* (14), 5843−5859.
(41) Fakih, S., Podinovskaia, M., Kong, X., Collins, H. L., Schaible, U. E., and Hider, R. C. (2008) Targeting the lysosome: fluorescent iron(III) chelators to selectively monitor endosomal/lysosomal labile iron pools. *J. Med. Chem. 51* (15), 4539−4552.
(42) Farard, J., Lanceart, G., Loge, C., Nourrisson, M. R., Cruzalegui, F., Pfeiffer, B., and Duflos, M. (2008) Design, synthesis and evaluation of new 6-substituted-5-benzyloxy- 4-oxo-4H-pyran-2-carboxamides as potential Src inhibitors. *J. Enzyme Inhib. Med. Chem. 23* (5), 629−640.
(43) Ma, Y., Luo, W., Quinn, P. J., Liu, Z., and Hider, R. C. (2004) Design, synthesis, physicochemical properties, and evaluation of novel iron chelators with fluorescent sensors. *J. Med. Chem. 47* (25), 6349−6362.
(44) Rosini, M., Simoni, E., Bartolini, M., Cavalli, A., Ceccarini, L., Pascu, N., McClymont, D. W., Tarozzi, A., Bolognesi, M. L., Minarini, A., Tumiatti, V., Andrisano, V., Mellor, I. R., and Melchiorre, C. (2008) Inhibition of acetylcholinesterase,β-amyloid aggregation, and NMDR receptors in Alzheimer's disease: a promising direction for the multi-target-directed ligands gold rush. *J. Med. Chem. 51*, 4381−4384.
(45) Tan, D. X., Manchester, L. C., Hardeland, R., Lopez-Burillo, S., Mayo, J. C., Sainz, R. M., and Reiter, R. J. (2003) Melatonin: a hormone, a tissue factor, an autocoid, a paracoid, and an antioxidant vitamin. *J. Pineal Res. 34*, 75−8.
(46) Tang, L., Zhao, L., Hong, L., Yang, F., Sheng, R., Chen, J., Shi, Y., Zhou, N., and Hu, Y. (2013) Design and synthesis of novel 3-substituted-indole derivatives as selective H3 receptor antagonists and potent free radical scavengers. *Bioorg. Med. Chem. 21*, 5936−5944.
(47) Shi, Y., Sheng, R., Zhong, T., Xu, Y., Chen, X., Yang, D., Sun, Y., Yang, F., Hu, Y., and Zhou, N. (2012) Identification and characterization of ZEL-H16 as a novel agonist of the histamine H3 receptor. *PLoS One 7* (8), e42185.
(48) Łażewska, D., and Kiec-Kononowicz, K. (2010) Recent advances in histamine H_3 receptor antagonists/inverse agonists. *Expert Opin. Ther. Pat. 20* (9), 1147−1169.

DOI: 10.1021/acschemneuro.5b00224
ACS Chem. Neurosci. 2016, 7, 69−81

(49) Geng, J., Li, M., Wu, L., Ren, J., and Qu, X. (2012) Liberation of copper from amyloid plaques: making a risk factor useful for Alzheimer's Disease treatment. *J. Med. Chem. 55*, 9146−9155.
(50) el-Jammal, A., Howell, P. L., Turner, M. A., Li, N., and Templeton, D. M. (1994) Copper complexation by 3-hydroxypyridin-4-one iron chelators: structural and iron competition studies. *J. Med. Chem. 37* (4), 461−466.
(51) Sharma, A. K., Pavlova, S. T., Kim, J., Finkelstein, D., Hawco, N. J., Rath, N. P., Kim, J., and Mirica, L. M. (2012) Bifunctional Compounds for Controlling Metal-Mediated Aggregation of the Aβ_{42} Peptide. *J. Am. Chem. Soc. 134*, 6625−6636.
(52) Tõugu, V., Karafin, A., Zovo, K., Chung, R. S., Howells, C., West, A. K., and Palumaa, P. (2009) Zn(II)- and Cu(II)-induced non-fibrillar aggregates of amyloid-beta (1−42) peptide are transformed to amyloid fibrils, both spontaneously and under the influence of metal chelators. *J. Neurochem. 110*, 1784−1795.
(53) Telpoukhovskaia, M. A., Rodriguez-Rodriguez, C., Scott, L. E., Page, B. D., Patrick, B. O., and Orvig, C. (2014) Synthesis, characterization, and cytotoxicity studies of Cu(II), Zn(II), and Fe(III) complexes of N-derivatized 3-hydroxy-4-pyridiones. *J. Inorg. Biochem. 132*, 59−66.
(54) Scott, L. E., Telpoukhovskaia, M., Rodriguez-Rodriguez, C., Merkel, M., Bowen, M. L., Page, B. D. G., Green, D. E., Storr, T., Thomas, F., Allen, D. D., Lockman, P. R., Patrick, B. O., Adam, M. J., and Orvig, C. (2011) N-Aryl-substituted 3-(beta-D-glucopyranosyloxy)- 2-methyl-4(1H)-pyridinones as agents for Alzheimer's therapy. *Chem. Sci. 2* (4), 642−648.
(55) Bolea, I., Gella, A., and Unzeta, M. (2013) Propargylamine-derived multitarget-directed ligands: fighting Alzheimer's disease with monoamine oxidase inhibitors. *J. Neural Transm. 120*, 893−902.

DOI: 10.1021/acschemneuro.5b00224
ACS Chem. Neurosci. 2016, 7, 69−81